Lithobiontic recolonization following cleaning and preservative treatments on the rock engravings of Valle Camonica, Italy: A 54-months monitoring

Graphical Abstract

Rock art of Valle Camonica

54 months monitoring (fluorimetry & colorimetry)

Before cleaning
After cleaning
After 2 months
After 13 months
After 25 months
After 37 months
After 49 months
After 54 months

different lithobionts

Mosses

Lichens

Cyanobacteria

different microenvironmental conditions

Benzalkonium chloride

Usnic acid

Benzalkonium chloride

Polysiloxane water repellent

Ethyl-silicate based consolidant

Plant essential oils

TiO_2

Nanocrystalline anatase

No preservative treatment

No preservative treatment

different cleaning
&
preservative treatments

Pre-cleaning devitalization of lithobionts

No pre-cleaning devitalization of lithobionts

Lithobiontic recolonization following cleaning and preservative treatments on the rock engravings of Valle Camonica, Italy: A 54-months monitoring

Highlights

Biofilms, mosses and lichens monitored by image analysis, fluorimetry and colorimetry

Effectiveness of preservative treatments dependent on microenvironmental conditions

Lowest after cleaning re-darkening with polysiloxane water repellent and nano-anatase

Delayed recolonization also with the application of synthetic and natural biocides

No change in lichen diversity but increased nitrophytic species after some treatments

Lithobiontic recolonization following cleaning and preservative treatments on the rock engravings of Valle Camonica, Italy: A 54-months monitoring

Sergio E. Favero-Longo[1,*], Enrica Matteucci[1,2], Samuele Voyron[1], Paola Iacomussi[3], Maria Giuseppina Ruggiero[4]

[1] Dipartimento di Scienze della Vita e Biologia dei Sistemi, Università degli Studi di Torino, Viale Mattioli 25, 10125 Torino, Italy

[2] Fondazione Centro per la Conservazione e Restauro "La Venaria Reale", via XX settembre 18, 10078, Venaria Reale (TO), Italy

[3] Istituto Nazionale di Ricerca Metrologica, Divisione Ottica, Strada delle Cacce 91, 10135 Torino, Italy

[4] Direzione Regionale Musei della Lombardia, Palazzo Litta, Corso Magenta, 24, 20123 Milano, Italy

*Corresponding author

Sergio Enrico Favero-Longo
Dipartimento di Scienze della Vita e Biologia dei Sistemi
Università degli Studi di Torino
Viale Mattioli 25, 10125 Torino, Italy
+39-011-6705972
sergio.favero@unito.it

Abstract

Both the indirect control of microclimate conditions and the direct application of preservative products to contrast stone bioreceptivity may contribute to limit lithobiontic recolonization of cultural heritage surfaces after cleaning interventions. However, the priority deserved by these different preventive approaches has still been poorly evaluated, particularly in outdoor environments. This work dealt with the engraved sandstone surfaces of the National Park of Rock Engravings of Naquane (Italy, UNESCO WHS), widely colonized by lichens, mosses and a dark cyanobacterial biofilm, and thus requiring frequent cleaning interventions to preserve their legibility for visitors and scholars. In particular, post-cleaning recolonization by the different lithobionts was seasonally monitored along 54 months in different zones of an engraved outcrop, primarily differing in levels of shading, on parcels exposed to nine different conservative treatments. These included (or not) a pre-cleaning devitalization of lithobionts and the post-cleaning application of biocidal (benzalkonium chloride, plant essential oils, usnic acid) and other restoration products (nanocrystalline anatase, polysiloxane-based water repellent, ethyl-silicate-based consolidant). The combination of surface image analyses, fluorimetric and colorimetric measurements showed that mosses and the cyanobacterial biofilm rapidly recolonized all the parcels in the more shaded zone, irrespective of conservative treatments. In the other areas, recolonization significantly differed depending on the treatment. The post-cleaning application of biocides determined the best results through two vegetative seasons, but only nanocrystalline anatase and the polysiloxane-based water repellent maintained the surfaces lighter than uncleaned controls along the whole monitoring period. Recolonization primarily proceeded by the uncleaned surfaces surrounding the parcels and, at least in the examined case of lichens, did not show substantial shifts in community composition, although some nitrophytic species increased their frequency. In conclusion, the effectiveness of preservative treatments to prevent a rapid recolonization of heritage stone surfaces appeared subordinate to the presence of microenvironmental conditions less favourable to lithobionts.

Keywords

biocides; cyanobacterial biofilms; lichens; preventive conservation; restoration products; stone bioreceptivity

1. Introduction

Lithobiontic colonization is a major cause of concern for the conservation of the outdoor stone cultural heritage. When considering a risk-based approach -increasingly proposed for the management of cultural heritage (Konsta and Della Torre, 2021)-, the risks posed by lithobionts to heritage surfaces depend on the probability and the consequences of their colonization. The probability of colonization is related to the surface bioreceptivity, that is the aptitude of a material to be colonized and, thus, with the totality of material properties that contribute to the lithobiontic establishment (Guillitte, 1995; Sanmartín et al., 2021a). Moreover, it equally relates to the environmental conditions, which may favour or not lithobiontic communities, depending on specific ecological requirements (Caneva et al., 2008). The consequences of colonization have been widely assessed, showing heterogeneous scenarios depending on the composition of lithobiontic communities, the substrate lithology and the macro- and micro-climate conditions, with the type of heritage surface also conditioning the actual impact in terms of material preservation and observers' perception (Favero-Longo and Viles, 2020). Lithobionts often promote stone biodeterioration (*sensu* Hueck, 1965) and contribute to decrease heritage surface durability, but at least in some cases bioprotective effects were demonstrated (Pinna, 2021). Whatever the effect on the material preservation, lithobiontic colonization may cause disfiguring and masking of rock surfaces, and thus exerts a remarkable impact on heritage works with fine-scale surface details, as in the case of rock art (Tratebas, 2004; Zerboni et al., 2022).

In terms of management, strategies to reduce system risks potentially deal with both event probability and consequences. In the case of the stone cultural heritage outdoor, restoration interventions generally aim to eliminate lithobiontic colonization and consequent deterioration processes, but they should also increasingly point to limit the probability of new negative events, as it may be the case of lithobiontic re-colonization, and to prolong the heritage life. With this regard, conservative strategies may include one or both of the following options to prevent lithobiontic colonization: the control of microclimate conditions of heritage surfaces, strongly related to

extrinsic factors, and the reduction of their bioreceptivity, which deals with intrinsic factors. Accordingly, although with considerable difficulties in the outdoor conditions, strategies of stone heritage conservation are increasingly considering the possibility to limit environmental factors favouring the establishment and activity of lithobionts, as surface wetness and nutrient availability, and some positive results were documented (Pinna, 2017). More traditionally, cleaning interventions on heritage stone surfaces involve the devitalization and removal of lithobiontic communities, but also the post-cleaning application of preservative products to protect surfaces from new deterioration processes; these products include biocides -often the same used in the previous devitalization step-, consolidants and water repellents (Pinna, 2017). The cleaning process itself can modify the bioreceptivity of a stone material (tertiary bioreceptivity), with respect to the original one in the fresh (primary bioreceptivity) or in the (bio-)weathered state (secondary bioreceptivity; *sensu* Guillite 1995). However, the permanent or semi-permanent integration of preservative products after the cleaning can even more strongly modify its bioreceptivity (quaternary bioreceptivity *sensu* Sanmartín et al., 2021a), with both decreasing or increasing effects. In this context, a huge number of products has been tested on a wide range of heritage surfaces, and the duration of their positive effects has been characterized in both laboratory and/or field conditions against certain lithobionts and in certain (micro-)climatic conditions. In particular, such investigations have proliferated during the last decade(s) because of the progressive ban of several chemicals which were traditionally used as biocides, and the consequent need of more environmentally compatible alternatives for the post-cleaning preservation, but also for the pre-cleaning devitalization step (Fidanza & Caneva, 2019; Cappitelli et al., 2020; Sanmartín et al., 2023). Advantages and drawbacks have been reported for each of several new approaches, ranging, *e.g.*, from physical devitalization methods, which avoid to leave toxic chemical residuals, but display technical limitations and potential stress effects on the rock substrates (Sanmartín et al., 2019; Favero-Longo et al., 2021), to the adoption of plant and microbial metabolites with biocidal activity, as plant essential oils, whose natural origin, however, does not exclude they are/may be

104 also toxic to humans (Cappitelli and Villa, 2021; Pinna, 2022). More in general, long term effects of
105 post-cleaning preservative treatments have received attention by professional restorers and heritage
106 managers from a long time, and may be possibly documented in reports and applied literature on
107 cultural heritage conservation. However, similar investigations are still poorly available in scientific
108 literature, and were rarely conducted by comparing different approaches and supported by
109 quantitative measures about lithobiontic colonization. A major unexplored point, in particular, deals
110 with the priority which may be given to address preventive strategies affecting the microclimate
111 conditions of heritage surfaces or reducing their bioreceptivity with the application of preservative
112 products.

113 In the case of open air rock art conservation, complaints by Tratebas (2004) on the absence of
114 adequate systematic studies and controlled experiments on the control of biodeterioration issues
115 have been partially balanced by several valuable investigations on both cleaning and preventive
116 strategies, but knowledge on the topic still appears minimal (Batarda Fernandes et al., 2022). In
117 Europe, *e.g.*, investigations on the site of Côa Valley (Portugal, UNESCO WHS 866bis)
118 documented environmental factors favouring the lithobiontic colonization of the local engraved
119 schists (Marques et al., 2014, 2016) and compared potency and limitations, in terms of
120 recolonization patterns, of cleaning interventions by mechanical tools, combined with traditional
121 chemical biocides, and by laser (Pozo-Antonio et al., 2021; Paz-Bermudez et al., 2023). In the
122 Rogaland County (Norway), the results of limiting tree shading and surface wetness and the
123 periodic application of ethanol (every one or two years) are monitored from two decades (Bjelland
124 and Kjeldsen, 2021). In the case of the site 'Rock Drawings in Valcamonica (Italy, UNESCO WHS
125 94)', including more than 140,000 engravings, projects started in 2010s to monitor the distribution
126 of rock panels and their state of conservation, including biodeterioration issues (Ruggiero et al.,
127 2021). Since 2017, lithobiontic colonization has been particularly investigated in the National Park
128 of Rock Engravings of Naquane (Capo di Ponte, Brescia), the hearth of the WHS, and the efficacy
129 of biocidal treatments used in the Park to devitalize lithobionts prior to their mechanical removal

was evaluated and compared with other biocide application protocols and alternative physical treatments with microwaves (Favero-Longo et al., 2021). Moreover, environmental factors favoring (re-)colonization after cleaning interventions, and the valuable effect of limiting surface wetness to prolong the cleanness, were experimentally evaluated (Favero-Longo et al., 2023). In the current work, the efficacy of several cleaning and preservative treatments to maintain an engraved rock of the Park in a clean(er) status was monitored for 54 months. The focus dealt with the recolonization by the main constituents of lithobiontic communities reducing the legibility of rock art, namely cyanobacterial-dominated biofilms, lichens and mosses. Assayed protocols encompassed the pre-cleaning biocidal devitalization of lithobionts, the mechanical cleaning, and the post-cleaning application of biocidal chemicals, of synthetic and natural origin, and other restoration products. In particular, the efficacy of nine different protocols, monitored combining observations with fluorimetric and colorimetric measures, was evaluated on three different zones of a single outcrop, primarily differing in shading levels and in the duration of wetness after rain events. We tested the null hypotheses that: (a) the lithobiontic community visibly (re-)colonize the cleaned surfaces within the monitored period; (b) the zones differing in microenvironmental conditions (z1/z3) do not show different recolonization patterns in terms of times, abundance, and dominant lithobionts; (c) recolonization is not different on surfaces where lithobionts were treated with a biocidal chemical before their mechanical removal; (d) recolonization patterns are not affected by the different preservative treatments (comparison of the nine different protocols, and controls); (e) lichen community recolonizing the cleaned surfaces is not modified in terms of richness and species composition.

2. Materials and methods

2.1. Study area

The study was carried out in the Rock Engravings National Park of Naquane, located in the middle part of Valle Camonica [Capo di Ponte, Brescia, Italy: UTM WGS84: 32T 604400 m E, 5097700 m

156 N; Fig. 1A]. Climate data from a nearby monitoring station (ARPA Lombardia, n. 129;
157 www.arpalombardia.it/Pages/Meteorologia/Richiesta-dati-misurati.aspx) indicated, in the period
158 2013-2016, av. winter and summer air temperatures of 2°C and 21°C, respectively and 1000 mm
159 rainfall yr^{-1}. The Park includes 104 engraved sedimentary outcrops, mostly sandstones, of the
160 Verrucano Lombardo formation (Upper Permian), characterized by high cohesion and low porosity
161 because of the precipitation of quartz cement in pores (Brack et al., 2008).

162 Assays and monitoring activities were performed on Rock 30 (Fig. 1B), for which no cleaning
163 interventions are documented since the start of their registration for the Park in early 1980s
164 (www.irweb.it). In particular, experiments were conducted in the upper part of the outcrop (approx.
165 11.5 × 1.5 m), delimited by vegetated ground upwards and a 20 cm wide channel on the rock
166 surface related to glacial erosion downwards.

167 Along this rock surface, facing West and characterized by glacial striations, some engravings and an
168 inclination of approx. 30°, 27 parcels approx. 25 × 25 cm were aligned, distanced by approx. 15-20
169 cm (Fig. 1C; Fig. 2A). The first set of nine parcels, in the southern side (z1), was more strictly
170 surrounded by shrub vegetation and shaded by trees at the southern extreme, contributing a
171 prolonged time of wetness after rain events with respect to the other zones; the second set, in the
172 central zone (z2), was open and rather distanced from vegetation upwards; the third set, in the
173 northern zone (z3), was covered by a *Pinus sylvestris* tree, but open to direct irradiation from the
174 South (Fig. S1). The different surface wetness was not instrumentally monitored, but, as a reference
175 term, it is worth noting that on measuring days in late March and mid-October which followed rainy
176 nights, surfaces in z2 and z3 generally dried before the subsequent evening, while surfaces of z1 did
177 not.

178

179

2.2. *Characterization of lithobionts*

In April 2018, before starting the experiment, lithobiontic cover was quantified for each parcel by, analyzing images, acquired with a portable photographic device, with the WinCAM Pro 2007d software (Regent's Instruments). In brief, according to Gazzano and colleagues (2009), color classes were assigned to the black microbial biofilm, mosses, *Xanthoparmelia* foliose thalli, and other lichens through a selection of representative pixels on the processed images. Thereafter, the software quantified the pixels belonging to each color class, and thus the different lithobiontic covers.

Each parcel was particularly surveyed for lichen diversity, also with the aid of a hand lens, collecting samples for each different *taxon*. Preliminary field identifications were thus checked in the laboratory by using the online keys published in ITALIC, the Information System of the Italian Lichens, version 07 (see Nimis & Martellos, 2020). Lichen nomenclature follows Nimis (2023).

Moreover, microscopy observations and metabarcoding analyses were performed on four samples of the black biofilm unaffected by cleaning and preservative treatments, taken at the boundaries between the three zones, at the upper and lower limit of the parcel alignment, in order to characterize its microbial diversity.

2.3. *Metabarcoding analysis*

Total DNA was extracted by means of the DNeasy PowerSoil Kit (Qiagen, Hilden, Germany) following manufacturer's instructions, and the quality and quantity of the extracted DNA was assessed using the ND-1000 Spectrophotometer NanoDropH (Thermo Scientific). 16S rDNA was amplified by PCR in triplicate, using 20 ng of DNA per sample and the primer set 515fB (GT-GYCAGCMGCCGCGGTAA) (Parada et al., 2015) and 806rB (GGACTACNVGGGTWTCTAAT) (Apprill et al., 2015) targeting the V3–V4 hypervariable region. PCR conditions were those reported

204 in Voyron et al (2022). PCR products were checked on 1% agarose gel, the three replicates were
205 pooled and purified by means of the Wizard SV Gel and PCR Clean-Up System (Promega) following
206 the manufacturer's instructions. Purified amplicons were quantified using the Qubit Fluorometer 2.0
207 (Thermo Fisher Scientific, Waltham, MA, USA). Amplicons were paired-end sequenced, using the
208 Illumina MiSeq technology (2 × 300bp), by IGA Technology (Udine). The bioinformatic analysis of
209 the raw sequences was achieved by means of the microbiome bioinformatics platform QIIME2
210 (Quantitative Insights into Microbial Ecology 2, version 2021.2) (Bolyen et al., 2019). Sequence
211 quality control and chimeras removal were achieved by means of the DADA2 plugin (Callahan et al.,
212 2016). The qiime vsearch cluster-features-de-novo plugin using 97% as the identity threshold was
213 used to generate the Operational Taxonomic Units (OTU) table. The taxonomic assignment of
214 retrieved bacterial communities was achieved using the Greengenes Databases v. 13_8 (McDonald
215 et al., 2012).

216 The dataset generated for this study is deposited in the NCBI Sequence Read Archive (SRA-NCBI;
217 https://submit.ncbi.nlm.nih.gov/subs/sra, accessed on 25/04/2023) under project accession number
218 PRJNA911483.

219

220 *2.4. Cleaning and preservative treatments*

221 In late April-mid May 2018, each set of nine parcels received a series of different conservative
222 treatments -performed by professional restorers operative in the site-, which included the cleaning
223 of the rock surface and the application of preservative products (Fig. 2B). In all the parcels,
224 lithobionts were mechanically removed, as follows: as a first step, mosses and foliose lichen thalli
225 were gently removed using a scalpel, and to the extent possible the thalline component (*sensu*
226 Favero-Longo et al., 2005) of crustose lichens; thereafter the rock surface was brushed to remove
227 the cyanobacterial-dominated biofilm and the epilithic residuals of lichens. In two out of the nine

228 different treatments (coded A-), such mechanical intervention was not preceded by the biocide
229 application to devitalize the lithobionts, and deionized water only was used during brushing
230 activity. The first one did not imply the application of products on the surface following the
231 mechanical cleaning (A-CON), the second included the brush application of benzalkonium chloride
232 (3% in water; CTS s.r.l., Altavilla Vicentina, Italy), a practice previously adopted in some cleaning
233 interventions in the Park (A-BAC). In the remnant assays (B-), lithobionts were preliminary treated
234 with Biotin R [N-octyl-isothiazolinone (3-5%), 3-iodoprop-2-ynyl N-butylcarbamate (10-25%) in
235 diethylene glycol butyl ether; CTS s.r.l.], diluted in white spirit (3%) according to manufacturer's
236 instruction and applied by brush. Brush application was selected as it was the method usually
237 adopted in cleaning interventions in the Park when biocides were used. Biotin R was selected -
238 although not previously used in the site- following a previous investigation on heritage sandstone
239 surfaces in Italy (Favero-Longo et al., 2017). This previous work had showed a good devitalization
240 effectiveness for this product, at least on one of the targeted epilithic lichen species, also in the case
241 of brush applications, while these latter had been ineffective in the case of other commercial
242 biocides. In the parcels exposed to the biocidal application, the mechanical removal was supported
243 by the application of NeoDes (50% quaternary ammonium salts, 25% isopropanol; CTS s.r.l.),
244 diluted in deionized water (5%). After the mechanical removal, this second group of parcels
245 received the following set of products with biocidal properties, applied by brush: benzalkonium
246 chloride (3% in water; CTS s.r.l.; B-BAC); essential oils of *Thymus vulgaris* L. (1%; Erbamea, San
247 Giustino, Italy) and *Origanum vulgare* L. (1%, Erbamea) prepared in Funori (1%) following
248 Devreux et al. (2015) (B-EOL); the lichen metabolite usnic acid (0.02 mM; Sigma-Aldrich), with
249 reported allelopathic properties against microbial biofilms (Gazzano et al., 2013; Ruggiero et al.,
250 2020), prepared in acetone (1%) (B-USN); nanocrystalline anatase (TiO_2, P25, Degussa, Essen; 1%
251 suspension in water), with photocatalytic properties and reported autocleaning activity (Fonseca et
252 al., 2010) (B-NTI). The following restoration products, which had been used after cleaning
253 interventions in the Park, were also assayed: the polysiloxane-based water repellent Silo 112

(aqueous dispersion 10% w/w; CTS s.l.r.; B-SIL), and the water repellent and consolidant Estel 1100, based on silicic acid ethyl esters and oligomeric polysiloxanes (CTS s.r.l.; B-EST). A parcel with no addition of preservative products after the preliminary devitalization and mechanical cleaning was also established (B-CON). In each of the zones, the different treatments were in the same order (from N to S: A-BAC, B-USN, B-BAC, B-SIL, B-EST, B-EOL, B-NTI, B-CON, A-CON); areas between the parcels, where the lithobiontic community was undisturbed, were used as negative control (N-CON). The application by brush, and likely the scarce porosity of the substrate (Favero-Longo et al., 2023), allowed to target each parcel with the selected product, avoiding contaminations between neighbouring parcels, and of the undisturbed areas between the parcels.

2.5. Fluorimetric monitoring of recolonization

Images of the parcels were periodically acquired from May 2018, immediately after the cleaning, and processed by WinCAM software to quantify the percentage cover of the different lithobionts, as previously described. However, except that for mosses, image analyses appeared rather ineffective to quantify recolonization trends at early monitoring time points. Recolonization of the cleaned parcels, in particular by phototrophic lithobionts, was thus seasonally monitored by fluorimetric measurements (Fig. 2C). Following a first measuring session in late July 2018, monitoring time points were distributed seasonally, in mid-October, late March and late June, until Autumn 2021. The measuring session of March 2020 was missed because of COVID-19 pandemic. Measures were obtained using a portable Handy-PEA (Hansatech Instruments Ltd., Norfolk, England; saturating light pulse of 1s, 1500 μmol $m^{-2}s^{-1}$, peak at 650 nm). Before the measurements, the parcels were sprayed with water and dark adapted using a black fabric. Measurements were performed avoiding the central hours of the day; in particular, during the Summer sessions, measuring was conducted very early in the morning and stopped when the rock surface started to warm.

On each parcel, measuring points were established and repeated at each monitoring time point by using a plastic mask with 30 numbered holes, sized to the hole of the measuring clip (diam. 4 mm) mounted on the Handy PEA sensor head. Coordinates of the measuring points on the mask (the same for all the parcels) were randomly extracted by Excel before starting the monitoring program. Points corresponding to fractures and holes were discarded, so that a number of 20-25 measures was finally available per each parcel per monitoring time point.

The maximum quantum yield (F_v/F_m) and the basal fluorescence (F_0) were considered as reference parameters to evaluate phototrophic recolonization, being informative on the photosynthesis functionality (Stirbet et al., 2019) and related to the chlorophyll *a* contents (Sanmartín et al., 2019), respectively.

Generalized linear models (GLMs) were used to ascertain the influence of the following factors on recolonization: interval from the cleaning intervention (<6 months, 6-18 m, 18-30 m, 30-42 m), season (Spring, Summer, Autumn), zone of the outcrop (z1-z3) and conservative treatment (A-BAC, B-USN, B-BAC, B-SIL, B-EST, B-EOL, B-NTI, B-CON, A-CON; N-CON). In detail, factorial ANOVAs were performed to detect significant differences in F_v/F_m and F_0 according to the different predictors. Moreover, significant differences in F_v/F_m and F_0 at different monitoring time points, between outcrop zones, and treatments were evaluated by ANOVA with post-hoc Tukey's test ($P<0.05$ as significant). All statistics were carried out with SYSTAT 10.2 (Systat Software Inc., San Jose, CA, USA).

2.6. Colorimetric monitoring and other assessments of recolonization

In June 2021 (37 months after the cleaning), fluorimetric measurements were combined with a colorimetric characterization of the parcels and of the surrounding uncleaned surfaces, performed by a portable spectrophotometer (Konica Minolta CM-23d) which was previously unavailable (Fig.

2C). The following conditions were adopted: measurement condition 8/d (specular component included and excluded), instrument acceptance area 12 mm. Additional parcels 40×40 cm were appositely established below the central parcel of each zone (one for z1 and z3, two for z2), where lithobionts were mechanically removed to have available freshly cleaned sandstone surfaces, suitable as controls (just cleaned parcels, JUC). Colorimetric measurements were carried out a second time in June 2022 (49 months after the cleaning).

Per each parcel, 5 and 9 measuring areas were established at the 2021 and 2022 monitoring time points, respectively, using a mask with circular holes sized to the instrument acceptance area. For each spot CIE L*a*b* color coordinates were calculated for 2° observer and CIE D65 reference illuminant (ISO/CIE, 2019). CIE D65 is the reference illuminant for the so called Natural Light at 6500 K Correlated Color Temperature (CCT), representative of the diffusing light comings from the sky. Since the parcels were mostly achromatic (different levels of greys up to dark black) the most informative values were L* values (Lightness). The difference in lightness among parcels was expressed as difference from L* values of uncleaned and unprotected surfaces ($\Delta L^* = L^*_{uncleaned} - L^*_{treated}$), separately considered for each zone; negative values were thus representative of the protection efficacy of the different treatments with reference to the uncleaned and unprotected surfaces.

The survey of specific lichen diversity performed before the cleaning operations was repeated in June 2021 (37 months after the cleaning) and November 2022 (54 months), through the careful observation by a hand lens of each parcel and the sampling of representative minimal fragments to check identifications in laboratory by microscopic observations and chemical assays (spot tests). Nevertheless, most of new thalli were left undisturbed to allow the continuance of the long-term monitoring of lichen recolonization.

3. Results

3.1. Lithobiontic colonization before and immediately after the cleaning

Before the cleaning, all the parcels were completely covered by lithobiontic colonization (Figs. 1B, 1D; detail of each parcel in Fig. S2). In particular, a black microbial biofilm showed average cover values around 70 % (z1, z3)- 80 % (z2), while average moss cover varied between 26 % (z1), 15 % (z3) and 10 % (z2). Lichens occurred in all the parcels, with higher average cover in z3 (17 %) than in z2 (7%) and z1 (2%). Differences were remarkable even between adjacent parcels, so that for all lithobionts differences between zones were not statistically significant.

Eleven lichen *taxa* were detected through the parcels before starting the experiments, including foliose (64%) and crustose (36%) species. Higher diversity and average values of specific frequency through plots characterized z3 (11 species, av. frequency 42%) and z2 (9, 50%) with respect to z1 (5, 30%). In particular, species of genus *Xanthoparmelia* (*X. conspersa, X. glabrans* and *X. angustiphylla*) were responsible for most of lichen cover in z2 and z3 (>70%). Xerophytic (*Rufoplaca arenaria, Candelariella vitellina, Circinaria caesiocinerea*) and mesophytic (*Fuscidea lygaea, Pertusaria flavicans*) crustose species also occurred, with *P. flavicans* particularly characterizing z1. Species typically found as epiphytic, widespread in the communities on the surrounding trees (*Candelaria concolor, Phaeophyscia orbicularis, Physcia adscendens*), were also widespread in z3.

Microscopy observations of biofilm samples showed a prominent presence of filamentous and coccoid cyanobacteria (Fig. 1E), with subordinate green algae, lichen primordia and non-lichenized fungi, primarily dematiaceous meristematic ones. Metabarcoding analyses (Table S1) confirmed Cyanobacteria as a dominant bacterial component in the biofilm (19% of reads), and characterized the co-presence of coccoid (45% of cyanobacterial reads, mostly Chroococcales, Xenococcaceae) and filamentous (primarily *Stigonema*, Nostocaceae, and *Leptolyngbya*, Pseudanabaenaceae) *taxa*. Proteobacteria (29% of reads, mostly Alphaproteobacteria, Rhodospirillales, and Acetobacteraceae)

351 and Firmicutes (14% of reads, mostly Clostridia, Clostridiales, and Clostridiaceae) were also
352 abundantly detected.

353 After the cleaning intervention, mosses and lichen thalli were not visible on the surface of the
354 parcels. Moreover, in z3 and z2, the surfaces of all the parcels were thoroughly clarified, suggesting
355 an effective removal of the black microbial biofilm. Some parcels of z1, instead, were still partially
356 dark even after an intense brushing, suggesting, at least for a part of the biofilm, an endolithic
357 behaviour and the impossibility of an effective mechanical removal. However, fluorimetric
358 measurements randomly performed through the parcels (as the systematic sampling had still not
359 been planned) on the day after the BiotinR application, before the mechanical cleaning, mostly
360 showed F_v/F_m values lower than 0.1 (85% of 70 measures).

361

362 *3.2. Visual observation and image analysis of recolonization patterns*

363 The monitoring of the parcels highlighted different recolonization patterns depending on both the
364 zones and the treatments (Fig. 3A-C). Such strong variability was visually appreciable, with z1 only
365 exhibiting a remarkable moss recolonization and a general disappearance of parcel boundaries
366 already within the second year of monitoring, and the parcels of z3 and z2 displaying different
367 levels of darkening (Fig. S2).

368 Image analysis quantified moss recolonization rates, which in z1 followed a linear increase and
369 recovered the original average cover values, higher than 20%, in the fourth year of monitoring (Fig.
370 3D). In z3 and z2, moss average cover through the parcels after the 54 months of monitoring was
371 still approx. 3% and 1%, significantly lower than before the cleaning intervention.

372 Images acquired at the different monitoring time points showed that the growth of thalli from the
373 external borders of the parcels was a first evident responsible of some recolonization on the cleaned
374 surfaces. The phenomenon was particularly observable in the case of *Xanthoparmelia* thalli,

375 including those cut with a scalpel during the mechanical removal, but some crustose species (*R.*
376 *arenaria*) also showed a similar behaviour in some parcels. The appearance of some lichen thalli far
377 from the parcel borders started to be recognizable in some images from the third year of monitoring
378 only (Fig. 3E-H), although some very small foliose thalli of the nitrophytic *Candelaria concolor*
379 had been already observed during fieldwork in the second year, particularly in z3, as well as small
380 groups of areolae of crustose species. Even at the last monitoring time point, however, total lichen
381 cover quantified for each parcel by image analysis was generally lower than 5%, with the exception
382 of A-BAC and A-CON in z3 and z2 (cover in the range 6-15%; Fig. S3), mostly due to the growths
383 from the external borders of the parcels and/or associated to the presence of fissures, depressions
384 and roughness along the parcel profile (see Fig. S2, e.g. A-BAC in z2, B-CON in z3). Average
385 lichen cover calculated per each zone after 54 months were 3.7%, 3.2% and 0.5% in z3, z2 and z1,
386 respectively.

387 Images also documented the progressive regrowth of the biofilm on the parcels, visualizing
388 differences between zones and treatments. However, these were quantified by fluorimetric and
389 colorimetric measurements (next sections) rather than by image analysis. Microscopic observations
390 of some biofilm samples punctually collected from the parcels at the end of the monitoring (54
391 months) confirmed cyanobacteria as dominant components (images not shown).

392

393 3.3. *Phototrophic recolonization traced by fluorimetric measurements*

394 GLM analyses of fluorimetric measurements (Table 1) showed the significant contribution of all the
395 considered factors on the variability of the F_v/F_m and F_0 values. In particular, the season and the
396 year(s) from the cleaning intervention were the main driving factors, with strongly higher F-ratios,
397 followed by the treatment and the zone.

Control measures on untreated surfaces particularly exhibited a strong seasonality of F_v/F_m values, with values increasing from March to June to October in all the monitored years and zones (Fig. 4A). In the case of the treated parcels, the median F_v/F_m values calculated for each zone were zeroed until the first year after the cleaning intervention, and for one and two seasons more for the z2 and z3 zones, respectively (Fig. 4B). Thereafter, the same seasonal pattern registered on untreated surfaces was observed, although values in z2 and z3 were significantly lower (statistics on Summer time points is displayed in Fig. 4B).

The monitoring of F_0 was informative on the gradual recolonization by the phototrophic lithobionts on the cleaned surfaces, particularly stressing the differences between the three zones. A limited seasonal increasing of F_0 values was recognized on control surfaces, but less marked than in the case of F_v/F_m (Fig. 4C). Differently, in the case of cleaned parcels, a progressive increasing was clearly recognizable for each zone from the first to the last monitoring time points (Fig. 4D). In z3, F_0 values were very low (medians <10) for the first two years, while some increasing was already detectable for z2 after the first year from the cleaning. In both z3 and z2, however, the values were significantly lower than those collected in untreated areas through all the monitoring time points. Differently, values in z1 were lower than those in uncleaned areas only at the first monitoring time point and were remarkably higher than those in z2 and/or z3 until the last year of monitoring, when all the F_0 values were similar, and generally equivalent to those measured in uncleaned areas.

The effects of the different treatments were evaluated for the overall and each of the outcrop zones, particularly focusing on F_0 values, which better expressed the gradual lithobiontic recolonization (Table 2A; Fig. S5).

By considering the overall zones (TOTAL in Table 2A), all treatments maintained F_0 values lower than those of uncleaned areas until October 2020 (29 months after the cleaning). Until October 2019 (17 months), B-EOL and, subordinately, B-USN and B-BAC showed the highest efficacy to limit F_0 increasing and to maintain the highest percentage of measuring points zeroed (i.e. F_0<10; Table

2B). Treatments not preceded by the biocidal application (A-BAC and A-CON) and the equivalent ones conducted after the preliminary devitalization (B-BAC and B-CON) did not show significant differences, although the median F_0 values of the former were higher at some monitoring time points. On October 2020 (29 months), all treatments showed similar values, while at successive monitoring time points B-NTI and B-EOL, and subordinately B-SIL and B-CON, displayed the lowest F_0 values. Also for these treatments, however, median F_0 values were higher than 20, and a very low number of measuring points was still zeroed (less than 10%), indicating the occurred recolonization. Some divergences between the treatments, however, were still detectable, appearing more durable in z3 and z2 with respect to z1.

In z3, all treatments maintained F_0 values lower than uncleaned areas until March 2021 (34 months) (Table 2A), and all out of B-SIL and A-BAC displayed more than 50% of measuring points zeroed until October 2019 (17 months) (Table 2B). B-CON, B-BAC and B-NTI particularly showed a high effectiveness, maintaining the lowest F_0 values at the last fluorimetric monitoring time point (41 months), but also other treatments (B-USN, B-EOL, B-SIL) displayed values lower than uncleaned areas. In z2, all treatments maintained F_0 values lower than uncleaned areas until October 19 (17 months), but significant differences were detected between the treatments, which were also confirmed at the subsequent monitoring time points (Table 2A). B-EOL and B-NTI displayed the lowest F_0 values through the whole monitoring period, but also B-CON displayed a similar result at the last time point. In both the z3 and z2 zones, only B-NTI parcels still displayed more than 5% of zeroed F_0 values after June 2020 (25 months) and no zeroed values were observed for the overall treatments at the last fluorimetric monitoring time point (41 months) (Table 2B).

In z1, some treatments already displayed F_0 values similar to those of the untreated areas at the first monitoring time point (2 months), and no treatment determined F_0 values lower than those of untreated areas from October 2020 (29 months) (Table 2A). At previous monitoring time points, until June 2020 (25 months), B-EOL and, subordinately, B-USN showed the lowest F_0 values and

448 the highest percentage of zeroed F_0 measures (Table 2B). It is worth noting that some zeroed values
449 characterizing z1 parcels at the last monitoring time points (particularly the A-CON parcel) were
450 also influenced by the accumulation of vegetal detritus which partially covered the lithobiontic
451 community, mostly entrapped in mosses, and was difficulty removable without disturbing the
452 ongoing recolonization dynamic.

453

454 *3.4. Colorimetric assessment of surface darkening*

455 Colorimetric measurements, started in June 2021 (37 months after the cleaning) and ended one year
456 later (49 months), were particularly remarkable for z3 and z2. CIE L*a*b* values highlighted
457 significant differences between parcels subjected to different treatments, evaluated with respect to
458 control surfaces which did not undergo to cleaning interventions (Fig. 5). On both monitoring time
459 points (37 and 49 months after the cleaning), NTI and SIL parcels in z2 and z3 zones showed L*
460 values significantly higher than those of uncleaned areas, meaning that NTI and SIL were still
461 lighter than uncleaned surfaces even after 49 months ($\Delta L^*_{UNCL\text{-}B\text{-}NTI} \cong -8$; $\Delta L^*_{UNCL\text{-}B\text{-}SIL} \cong -3$; Fig. 5B).
462 Accordingly, their boundaries were still visually distinguishable (Fig. S2). In z3, B-BAC and A-
463 BAC also maintained advantages in L* values with respect to uncleaned areas until June 2022
464 ($\Delta L^* > -3$; Fig. 5B). B-BAC and A-BAC parcels in z2 and all the remnant parcels in both the zones
465 (excepted the mentioned NTI and SIL) showed L* values not significantly different from the
466 uncleaned and unprotected surfaces, thus generally appearing at the same level of darkness.
467 Nevertheless, already in June 2021, even the lightest B-NTI parcels were just perceivable darker
468 than JUC parcels in z2 and clearly darker in z3 (Fig. 5A).

469 In z1, the widespread moss growth prevented the collection of at least five measures per parcel and
470 a confident statistical comparison with the other zones. Average moss cover after 54 months in
471 parcels of z1 was higher than 35 %, spreading well beyond the fissures characterizing the parcel

surfaces. Nevertheless, beside the moss colonization, a different color pattern was generally recognizable in June 2021 with respect to the other zones. Noticeable ΔL* differences with uncleaned surfaces, with advantage in the lightness of treated parcels, were observed for B-CON ($\Delta L^*_{UNCL\text{-}B\text{-}CON} \cong -5$) and A-CON ($\Delta L^*_{UNCL\text{-}A\text{-}CON} \cong -9$), associated to a strong increasing of b*, visually revealed by a general greening of the parcels with reference to the uncleaned surfaces (Fig. S6). For all the other treatments, ΔL were > 0, indicating a similar or even greater darkening in the parcels than in the surrounding uncleaned surfaces.

3.5. Specific patterns of lichen recolonization

Re-surveys of lichen diversity after 37 and 54 months from the cleaning displayed recolonization by the same *taxa*, with all the previously listed species being detected at least in two parcels and only a primary thallus of *Cladonia* additionally appearing in one parcel (Table 3). Some recolonization was recognized for both *X. conspersa* and *X. angustiphylla*, but the sparse occurrence of a high number of very small thalli of these greenish Xanthoparmelias, at least in some parcels, prevented to fully trace their new distribution by chemical analyses, and they were thus considered altogether.

After 37 months, 89% of parcels already showed lichen recolonization (Table 3A) and the number of specific counts through the overall parcels was 49, i.e. 58% of the overall specific counts (84) at T_0 (Table 3D). After 54 months, all the plots displayed lichens (out of one in z1, where lichens observed after 37 months had been cancelled by mosses; Table 3A), and the number of specific counts further increased to 75, i.e. 89% of the T_0 counts (Table 3D). In most cases, they corresponded to the regrowth of *taxa* in the same parcels where they previously occurred (59%), while new growths were less frequent (41%) (Table 3B). With this regard, images acquired at the different monitoring time points showed that some crustose thalli regrew on the same surfaces occupied before the cleaning, and the same was observed for some green *Xanthoparmelia* thalli

(Fig. 3H). In other cases, however, thalli developed on different surfaces (e.g. crustose lichens on surfaces previously occupied by *Xanthoparmelia*; Fig. 3G). In 46% of cases, a *taxon* previously occurring in a parcel disappeared, but this trend was not similarly distributed for all the *taxa* (Table 3C). In particular, the frequency of greenish Xanthoparmelias through the plots remarkably decreased (from 74% to 33%), as well as that of *X. glabrans* (from 37% to 7%). The frequency of species usually found as epiphytic remarkably increased (*Candelaria concolor* +100%, *Phaeophyscia orbicularis* +150%, *Physcia adscendens* +30%). The most widespread crustose species at T_0, *Circinaria caesiocinerea* and *Fuscidea lygaea* (undistinguishable at the level of new areolae/early developed thalli without their sampling, and thus considered altogether), only disappeared in one out of 15 parcels and colonized four additional parcels (frequency +20%), and a similar expansion also characterized *Rufoplaca arenaria* (frequency +23%), while a decreased frequency was observed for *Candelariella vitellina* (-60%) and *Pertusaria flavicans* (-50%).

With respect to the different zones (Table 3d), after 54 months, regrowth in the same parcels (60% of initial counts confirmed) prevailed on the taxon disappearance (40%) in z3, where the occurrence of species usually found as epiphytic was more remarkable. A similar pattern, but related to a lower number of *taxa* and counts at T_0, characterized z1, while specific reports in z2 confirmed after 54 months (41%) were less than those non confirmed (59%). In z3 and z2, only some control parcels (A-CON, B-CON) and A-BAC showed an increase of specific diversity, while a decrease was detected in both the zones for B-BAC, B-SIL-B, B-EST and B-EOL parcels. In z1, B-EOL and B-BAC confirmed the diversity decrease, but the dynamic observed through the zone seemed primarily influenced by moss recolonization. With respect to the specific behaviour (Table 3b), it is worth noting that regrowth of greenish Xanthoparmelias mostly characterized parcels non treated with biocides before the cleaning (A-BAC, A-CON) and those pre-devitalized and then treated with usnic acid (B-USN). Similarly, *Candelariella vitellina* only recolonized A-CON and A-BAC parcels. New appearance of species usually reported as epiphytes in z3 and z2 particularly

521 characterized parcels treated with benzalkonium chloride (B-BAC and A-BAC; 75%), but this
522 pattern was not confirmed in z1, where they also appeared following other treatments.

523

524 **4. Discussion**

525 Recognition and knowledge of variables which may crucially influence the effectiveness and
526 durability of stone cleaning, including protocols adopted to remove lithobionts and/or
527 environmental factors, are expected to improve management practices in rock art sites (Batarda
528 Fernandes et al., 2022; Favero-Longo et al., 2023). In this framework, with respect to the five
529 hypotheses tested in this work, (a) lithobionts largely recolonized the cleaned surfaces within the
530 monitored period of 54 months (null hypothesis confirmed; see sub-section 4.1). (b) Adjacent zones
531 of the examined outcrop, differing in shading levels and in the duration of wetness after rain events,
532 showed different recolonization patterns in terms of times, abundance and dominant lithobionts
533 (null hypothesis rejected; see 4.2). (c) The monitored rock-art surfaces did not register systematic
534 differences in lithobiontic recolonization where the same treatment was preceded or not by the
535 application of Biotin R (null hypothesis confirmed, but see 4.3 on the poor devitalization
536 effectiveness of the biocide application by brush). (d) The post-cleaning application of biocidal
537 chemicals and other restoration products was a significant driver of different recolonization patterns
538 (null hypothesis rejected; see 4.4), although microenvironmental conditions more favourable to
539 lithobionts were sufficient to cancel the effectiveness of preservative treatments observed at the
540 distance of few meters. (e) After the cleaning interventions, the lichen community did not show any
541 drastic shift and was generally responsible for the recolonization observed throughout the parcels
542 (null hypothesis partially confirmed; see 4.5). However, nitrophytic species primarily found as
543 epiphytes appeared favoured after the cleaning and an increase in species richness particularly
544 followed some treatments (A-CON, B-CON, A-BAC) (null hypothesis partially rejected). Such

545 main findings and operative insights on the assayed treatments for the preventive conservation of
546 heritage surfaces, and rock-art in particular, are hereafter discussed.

547

548 *4.1. Recolonization time of the lithobiontic community*

549 *In situ* investigations on recolonization dynamics are still scarce in scientific literature, often
550 adopted different quantification approaches and rarely followed the processes for more than one
551 year, thus limiting the availability of comparable information; reports by restorers widely document
552 recolonization phenomena, but as qualitative assessments rather than with quantitative measures. In
553 this study, although differences were recognized between the different zones and treatments (see
554 subsequent sub-chapters), recolonization was already detected few months after the cleaning, and
555 three years were sufficient to make lithobionts, and the cyanobacterial biofilm in particular, largely
556 re-established, with a consequent effect in terms of re-darkening, as documented by colorimetric
557 measurements. Such recolonization in the turn of (few) years agree with the practical approach to
558 repeat ethanol applications every one or two years on engraved rocks in Norway (Bjelland and
559 Helberg, 2006; Bjelland and Kjeldsen, 2021). Oppositely, schists of the rock art site of Côa in Spain
560 were still widely uncolonized after four years from a cleaning intervention including the application
561 of synthetic chemical biocides (Pozo-Antonio et al., 2021). One year was insufficient to allow a
562 perceivable recolonization by an algal biofilm on a vertical granite wall of a semi-enclosed
563 environment, irrespective of different cleaning treatments (Sanmartín et al., 2020), but in another
564 case study, dealing with an algal biofilm in a cave, recolonization of a cleaned parcel was already
565 clearly recognizable after twelve months, starting from the uncleaned adjacent areas (Borderie et al.,
566 2014). Analogously, the abundance of viable lithobionts at the immediate borders of the parcels
567 appeared as a driver of rapid recolonization, particularly visualized by the frequently observed top
568 down direction of re-darkening process. A similar recolonization pattern was related to the regrowth
569 of the foliose thalli of *Xanthoparmelia* species which were cut during the cleaning operations.

570 Lichen cover, however, was only poorly re-established at the end of the monitoring period. A
571 complete recovery of lichen cover was documented in the case of calcareous statues after eight
572 years from the cleaning, despite of treatments with water repellents (Nascimbene et al., 2009); in
573 the case of stone surfaces treated with combinations of water repellents, consolidants and biocides,
574 lichen recolonization started after 6 years, while dematiaceous fungi had already appeared 10
575 months after the cleaning (Pinna et al., 2018). Following the restoration of a church façade,
576 cyanobacteria and mosses rapidly recolonized the cleaned mortar surfaces, in the turn of few
577 months, while lichens did not (Jurado et al., 2014). Similarly, cyanobacteria, and also mosses, were
578 the primary responsible for the recolonization of the cleaned parcels.

579 The season and the time interval from the cleaning (years) were the primary drivers of the
580 variability of maximum quantum yield (F_v/F_m) and the basal fluorescence (F_0), prevailing on the
581 effects of treatments and zones, and thus indicating a significant relationship between the
582 lithobiontic growth and mesoclimate conditions, and a certain ineluctability of the recolonization,
583 respectively. A seasonality of fluorimetric values was previously documented for both
584 cyanobacteria and lichens, and related to changing levels of sun irradiation and available water
585 (Bowker et al., 2002; Baruffo and Tretiach, 2007). In particular, previous investigations already
586 detected the highest values of F_v/F_m and F_0 in fall, possibly due to the combination of higher water
587 availability and a shorter photoperiod, allowing a better recovery from photoinhibition and higher
588 production of chlorophyll (Bowker et al., 2002; Baruffo and Tretiach, 2007). Data from the closest
589 meteorological station confirmed for all the monitored years higher humidity and lower irradiation
590 values for October with respect to those registered in March and June (average values of RH and
591 irradiation, calculated per month, in Table S2). Different availability and length of periods
592 climatically favourable to the growth of phototrophic lithobionts may contribute to explain the
593 different times of recolonization reported for heritage sites in different geographical areas.
594 Moreover, the obtained results remark the necessity of comparing results obtained in the same
595 seasonal conditions when analyses of treatment efficiency and monitoring of lithobiontic

596 recolonization are based on fluorimetric measurements. Nevertheless, in the case of the treated
597 parcels, the progressive increase of F_0 values from the cleaning intervention to the last monitoring
598 time point on October 2021 remarkably prevailed on the seasonal trend, and documented the fast
599 recolonization of the sandstone surfaces.

600

601 *4.2. Recolonization and the different microenvironmental conditions of the three monitored zones*

602 Meso- and microclimate conditions control the composition of lithobiontic communities on rock
603 surfaces, and were shown to regulate their biodeterioration impacts just in the peculiar case of
604 engraved rocks (Marques et al., 2014, 2016). The presence of plant vegetation, which shades the
605 rock surfaces, decreasing temperature and increasing humidity, and provides nutrients, particularly
606 contributes to shape the lithobiontic colonization on heritage stone surfaces (Caneva et al., 2008,
607 2015). Different levels of shading and surface wetness duration after rain events distinguished the
608 parcels of the three monitored zones, where different colonization patterns were originally
609 surveyed, before the cleaning, and different recolonization dynamics were then observed. The
610 original prevalence of the dark cyanobacterial biofilm in z2, more distanced from higher plants and
611 thus more xeric, and a remarkable moss cover in the more sheltered and humid z1, with z3 as an
612 intermediate condition, reflected relationships between microenvironmental conditions and the
613 composition of lithobiontic communities generally reported in archaeological and monumental sites
614 through the world (e.g. Rishbeth, 1948; Caneva et al., 2015). Shading conditions had been also
615 associated to increased recolonization rates after cleaning (Delgado Rodrigues et al., 2011;
616 Salvadori and Charola, 2011). In our work, we experimentally showed that, in absence of any
617 intervention on the microenvironmental conditions of the examined rock outcrop, the original
618 patterns of lithobiontic distribution were generally re-established, with a fast moss recolonization
619 prevailing in z1, the cyanobacterial community widely recovering in z2 and z3, and (see detailed
620 discussion in sub-chapter 4.4) some higher lichen presence in few parcels of z3 and z2. More

621 remarkably, in the case of z1, the influence of the favourable microenvironmental factors generally
622 prevailed on that of the treatments, as quite no difference was recognizable already after 29 months
623 between all the parcels, which turned blackened and rich of moss cover similarly to uncleaned
624 control areas. Some durable divergence between treatments was instead visually and instrumentally
625 recognizable in z2 and z3, at a few meters of distance, remarking the unsuitability of selecting a
626 certain conservative treatment or approach on the basis of assays performed in a different site (or in
627 the laboratory). Moreover, comparative assays of the effectiveness of treatments to reduce surface
628 bioreceptivity and preserve surface cleanness may be unjustified if microenvironmental factors
629 driving an ineluctable rapid recolonization are not preventively controlled or mitigated. In
630 particular, these findings remark the crucial role of plant vegetation control around engraved rock
631 surfaces to avoid prolonged moist conditions, long recognized as a crucial conservation practice in
632 the management of Norwegian rock art (Bjelland and Helberg, 2006), but not generally adopted.
633 The possibility to protect engraved rocks from groundwater run-off, and thus reduce conditions
634 favourable to cyanobacteria, was also attempted (Young and Wainwight, 1995). This approach of
635 limiting prolonged water fluxes on engraved surfaces was also recently assayed on another outcrop
636 of the National Park of Naquane (Rock 70), in combination with the reduction of tree cover,
637 successfully zeroing cyanobacterial recolonization at more than three years from the cleaning
638 intervention (Favero-Longo et al., 2023).

639

640 *4.3. Recolonization and the preliminary biocide treatment applied by brush*

641 Investigations on the effectiveness of biocidal treatments have clarified the crucial importance of
642 the application tool, generally showing a high performance of strategies prolonging the wetness of
643 the target organisms and, thus, their metabolic activity and sensitivity to active principles, as for
644 biocide applications with poultices (Favero-Longo et al., 2017; Gallo et al., 2020). In comparison
645 with poultice applications, those by brush display lower effectiveness, not promoting a prolonged

wetness, but also providing a lower biocide amount (Favero-Longo et al., 2020); nevertheless, they are mostly adopted in the practical activity of restorers, due to the shorter time needed and lower costs. Accordingly, the poor difference in recolonization patterns observed between parcels which only differed for the preliminary devitalization treatment by Biotin R likely relates with a poor effectiveness of the application tool, chosen to simulate previous restoration activities in the National Park. In previous studies in other heritage sites Biotin R had shown some effectiveness against lithobionts also when applied by brush, generally higher than other products (Bartolini et al., 2007; Favero-Longo et al., 2017), while in other cases its application on crustose lichens followed by mechanical had left remains of thalli still including few viable photobionts (de los Ríos et al., 2012). Assays performed on the engraved rocks of Naquane in spring 2018 [in parallel with this study, due to practical constrains] showed an incomplete efficacy against both crustose and foliose lichens, and even against the cyanobacterial biofilm, displaying a good recovery of photosynthetic yields after 40 days from the treatment (Favero-Longo et al., 2021). Such result justifies the rapid recovery of F_v/F_m and F_0 values observed in some parcels already after a couple months from the treatment, particularly in the case of z1 where the mechanical action was visibly unable to cancel the darkened appearance of some parts of some parcels (Fig. S2), possibly due to some (chasmo-)endolithic growth of cyanobacteria, locally observed on other outcrops of the heritage site (Favero-Longo et al. 2023). Although some effects were recorded with respect to lichen regrowth (see sub-chapter 4.4), the performed experiment was thus poorly informative on the actual recolonization on parcels which received an effective devitalization treatment, also where Biotin R was applied (B-parcels). It rather documented the performance of preservative treatments in the difficult (but usual) condition of a poorly effective biocide application by brush, where the immediate result of cleaning in terms of visual appearance, but also of F_v/F_m and F_0 zeroing, mostly depends on the mechanical removal of lithobionts. Moreover, the poor results of the Biotin R application confirmed the difficulty of translating the results obtained on biocide effectiveness in a certain site against a

671 certain target species to another case study, and the importance of preliminary ad-hoc assays to
672 address suitable devitalization treatments (Favero-Longo et al. 2017; Sanmartín et al., 2023).

673

674 *4.4. Recolonization and the different preservative treatments*

675 Microenvironmental conditions of z3 and z2, less favourable to the rapid biofilm recolonization and
676 the abundant growth of mosses observed in z1, allowed to appreciate and compare differential
677 performances of the different preservative treatments.

678 On the basis of colorimetric measurements after 37 and 49 months, the application of
679 nanocrystalline TiO_2 (B-NTI) and, subordinately, the polysiloxane-based water repellent (B-SIL)
680 determined the best results in limiting the re-darkening of the sandstone surfaces. Lower plant cover
681 on NTI parcels in both z3 and z2 likely contributed to activate the photoinhibitory effect of the
682 product (Fonseca et al. 2010), not observed in the more shaded z1 parcel. The lowest F_0 values
683 quantified after 41 months indicated that the chromatic divergence from the other parcels was not
684 (only) due to the white color of the applied product. It is worth to remark that, although the product
685 gave positive results in preventing recolonization, its application implied the addition of a mineral
686 exogenous component which cannot be removed from the stone surface and thus determined a
687 permanent modification, likely undesirable. On the other hand, although in this work a white
688 nanocrystalline anatase was used, some other photoinhibitory nanoproducts were shown to not
689 significantly affect the color of the treated surfaces (Goffredo et al., 2017). Application of water
690 repellents, including polysiloxanes, already showed the capacity of delaying for several years the
691 recolonization of treated surfaces, their influence resulting more important than that of biocides
692 used in preliminary devitalization treatments, which are rinsed (Salvadori and Charola, 2011). A
693 durable protective effect was particularly observed for water repellents combined with copper
694 nanoparticles (Pinna et al., 2018), while in this experiment polysiloxanes only (i.e. triethoxyoctyl-

695 silanes of SIL) were responsible for a reduction of sandstone bioreceptivity with respect to other
696 parcels (out of NTI), suggesting some physical modification of microenvironmental conditions,
697 likely dealing with water availability, rather than chemical inhibition. However, an opposite effect
698 was instead observed with the application of oligomeric polysiloxanes combined with silicic acid
699 ethyl esters (B-EST), determining a rapid recolonization pattern and even a higher darkening than
700 surrounding uncleaned areas; that is a result in agreement with the observation of a favouring role
701 of the surface cracking of other ethyl-silicate based products, determining high water retention and
702 microbial anchoring (quaternary bioreceptivity; Sanmartín et al., 2021b), and which further remarks
703 the importance of testing the effects of each restoration product.

704 Parcels treated with the biocidal products, including the synthetic benzalkonium chloride (BAC)
705 and the natural compounds usnic acid (USN) and essential oils (EOL), recovered more rapidly than
706 B-NTI and B-SIL high F_0 values and a darkened appearance, which after 37 months was not
707 significantly different from the uncleaned control surfaces. Nevertheless, B-EOL parcels of z3 and
708 z2 showed the lowest F_0 values and the highest number of zeroed F_0 values until the 17^{th} month of
709 monitoring, followed by B-BAC and B-USN. Several papers recently documented the biocidal
710 effect of several plant essential oils against microbial biofilm constituents (Caneva and Fidanza,
711 2019), including cyanobacteria (Gabriele et al., 2023) and lichens (Favero-Longo et al., 2022).
712 Their inhibitory effects were mostly demonstrated in laboratory experiments, and some studies also
713 documented *in situ* their potency as natural biocides to devitalize lithobionts before their removal
714 and/or their support to cleaning operations (e.g. Spada et al., 2021). Similarly, inhibitory effects of
715 usnic acid against cyanobacteria had been demonstrated in laboratory conditions (Gazzano et al.,
716 2013; Ruggiero et al., 2020). Our results showed that the application of EOL and USN on the
717 sandstone parcels contributed to maintain the cleaning state along two vegetative seasons, as far as
718 BAC. Such result may lie in the fact that all these biocidal applications finalized the devitalization
719 of lithobiontic residuals that the brush application of Biotin R had failed to reach and the
720 mechanical action to remove. This interpretation would underline the importance to constantly

include a double devitalization treatment in cleaning protocols, before and after the mechanical removal of lithobionts. Accordingly, on schists of the rock art area of Côa, parcels treated with synthetic chemical biocides, including benzalkonium chloride and the isothiazolinone-based Biotin T, applied by brush, but repeated two times -before and after the mechanical removal of lithobionts-, still appeared largely clean at four years from the intervention (Pozo-Antonio et al., 2021). Similar processes could be independent from the fact that the water soluble biocides, as BAC, may be easily washed away after its application, preventing a long term preservative effect, as also supposed for other water soluble compounds (Li et al., 2020). However, absorption of biocides (including BAC) by rock substrates was also documented, creating a stock and favouring long term emissions, which may prolong the inhibitory effects (Gromaire et al., 2015). Such processes, which appear as the natural counterpart of long-term releasing biocidal products (Trojer et al. 2015), depend on the mineralogical and physical properties of the stones (Young et al., 1995). Preliminary assays on freshly cut slates of Verrucano sandstones showed a lower BAC absorption and a higher washing off with respect to other sandstones, likely related with a low clay content and scarce porosity (Favero-Longo et al., 2020), but measures should be more properly extended to the weathered upper crust of the engraved surfaces and also consider EOL and USN. For the latter, some persistence at the rock surface should not be excluded due to its negligible water solubility, but this secondary metabolite, acting photoprotection in many lichen species, was shown to be broken down by UV in photoproducts of lower molecular weight (Begora and Fahselt, 2001), suggesting that it could not remain as a protective stock on the upper sun-exposed surfaces, but rather within internal rock discontinuities. Uncertainty on the product durability and stability and, mostly, the observation of a prominent recolonization after two years only suggests that scientific investigations comparing the effectiveness of (alternative) preservative products should extend on a time scale longer than that of six months or one year which many of recent experiments considered. From a practical point of view, the protective effects of USN and EOL, although limited in time, may be renewed by a periodical application every 18-24 months, addressing a preventive approach of conservation by

747 reducing the bioreceptivity of engraved surfaces, rather than making necessary a full cleaning
748 intervention after a prominent lithobiontic recovery within a (slightly) longer period.

749 Parcels which did not receive any preservative treatment (B-CON) also displayed some of the
750 lowest F_0 values, in both z3 and z2. However, they displayed a low percentage of measuring points
751 with zeroed F_0 already after few months and, after 41 months, they were darkened as well as
752 surrounding uncleaned areas. Such misfit suggests that some modification in the lithobiontic
753 microbial community may have happened, as in the case of other heritage surfaces (Sanmartín and
754 Carballeira, 2021), with a higher recolonization by fungi and lower cyanobacterial dominance than
755 in other parcels. However, such analysis goes beyond the aim of the present work and will be part
756 of a separate paper including molecular analyses of the novel microbial community (Favero-Longo
757 et al., in preparation).

758

759 *4.5. Recolonization and lichen diversity*

760 Investigations on lichen recolonization of heritage stone surfaces after restoration interventions
761 documented remarkable shifts in specific composition, with a simplified community structure and a
762 dominance of nitrogen-tolerant species being prominent features (Nascimbene et al., 2009). In the
763 examined case, a similar shift was not observed, but the poorness of species and the presence of a
764 remarkable nitrophytic component indicated a condition of disturbance for saxicolous lichen
765 colonization already before the cleaning of the parcels. This was possibly related to old cleaning
766 interventions, not documented after early 1980s, in the period covered by archive documentation
767 (irweb), but carried out on most of the rocks of the Park in previous decades; moreover, in the last
768 70 years, following the establishment of the National Park in 1955, the whole area was shifted from
769 a grassland open habitat to a (managed) forest (Favero-Longo et al., 2023). In this framework,
770 foliose nitrophytic species typically associated to epiphytic communities were the first responsible

771 of lichen recolonization, showing the highest frequency increases through the parcels, with their
772 spread likely favoured by the shared and effective, clonal reproduction by asexual propagules
773 (soredia), which do not need the re-establishment of the symbiosis (Scheidegger and Werth 2009).
774 Their recolonization of the parcels thus appeared strictly related to the proximity of thalli diffusing
775 the symbiotic propagules from the surrounding trees. Typical saxicolous species, instead, generally
776 decreased their frequency, particularly in the case of foliose species of genus *Xanthoparmelia*.
777 Accordingly, foliose species, which discontinuously contact and poorly penetrate the rock substrate
778 with their rhizines, are more easily removed by restorers with mechanical tools, while crustose,
779 more penetrating species represent a more difficult task (Pinna, 2017). With this regard, the poor
780 effectiveness of the preliminary devitalization treatment by Biotin R likely allowed the persistence
781 of viable residuals, on the surface and/or in the penetrated rock discontinuity, which may have then
782 favoured the widespread reappearance of the same species in the same parcels (from 40 to 60% of
783 confirmed specific presences in the parcels, depending on the zone) and also, at least in some cases,
784 of thalli in the same positions, often related to rock fissures. Recolonization by crustose lichens
785 observed after four years on schists treated with chemical synthetic biocides in Spain was
786 particularly associated to discontinuity related to schistosity planes (Pozo-Antonio et al., 2021).
787 However, brush applications of Biotin R followed by mechanical cleaning were shown to exert an
788 effective devitalization of the hyphal penetration component of lichens (*sensu* Favero-Longo et al.
789 2005), while already displayed some partial effectiveness in the removal of epilithic thalli, possibly
790 leaving viable remains (de los Ríos et al., 2012).

791 Although the scarce success of the Biotin R application was not expected at the beginning of the
792 experiment, this contributed to show the limits of interventions lacking an effective preliminary
793 devitalization, which cannot be fully balanced by additional preservative treatments. Nevertheless,
794 some effects of these latter and the preliminary devitalization were recognizable, as just parcels A-
795 CON and B-CON, not receiving any preservative product, and A-BAC displayed the highest
796 increases of lichen specific frequencies. Moreover, parcels A-BAC and A-CON in z3 and z2

displayed the highest lichen cover values after 54 months. Similarly, in the case of schists of the Spanish rock art site, surfaces cleaned by water only displayed a deep lichen recolonization (Paz-Bermùdez et al., 2023). In the peculiar case of greenish Xanthoparmelias, the observed regrowth of thalli characterized, with one exception, parcels which did not receive the preliminary devitalization and/or preservative treatments, but also those treated with usnic acid, that they also produce (Nimis, 2023) and thus are expected to tolerate. The new growths of epiphytic foliose species in z2 and z3, mostly associated to parcels treated with benzalkonium chloride (75% of cases), deserve particular attention, as the use of quaternary ammonium salt was supposed and often reported to promote the colonization by nitrophytic species, serving as nutrients (Scheerer et al., 2009), but experimental support about this pattern is still poor. Our finding contributes some support to this hypothesis; however, we have to remark that, due to the reduced number of replicates, the relative positions of BAC parcels with respect to the trees surrounding the examined outcrop the could have also been influent.

5. Conclusions

In conclusion, this work experimentally showed that the evaluation of the effectiveness of treatments to control lithobiontic recolonization after a cleaning intervention, here examined on an engraved sandstone outcrop, needs to consider their impact on the rock bioreceptivity with careful reference to the microenvironmental conditions of interest.

Along the 54-months of monitoring, recolonization by mosses, lichens and the cyanobacterial biofilm previously occurring on the rock surface resulted ineluctable, but some factors were particularly related to a high recolonization/poor restoration success. (i) The persistence of microenvironmental conditions favouring one or more lithobiontic (micro-)organisms made locally insignificant every preservative treatment, as observed in the case of the rapid recolonization by the

821 black biofilm and mosses in z1, characterized by a higher shading level and longer duration of
822 wetness after rain events. (ii) The occurrence of viable lithobiontic communities in the nearby of the
823 cleaned surfaces was responsible to restart the colonization by water dispersal and/or propagule
824 release (Morando et al., 2019), as in the case of the black biofilm diffusing from the external
825 borders of the cleaned parcels and of nitrophytic lichens deriving from the epiphytic communities
826 on the surrounding trees. Although the possibility to modulate these factors may also depend on
827 management choices beyond the stone conservation issue -which in the study case deal with the will
828 to maintain the managed forest scenario of the National Park- their consideration appears an
829 essential priority to reduce the risk of rapid recolonization after cleaning. In particular, conservation
830 studies may contribute to experimentally validate intervention strategies and/or good practices to
831 obtain and maintain microenvironmental conditions less favourable to lithobionts, encompassing
832 the management of canopy cover (shading, presence of nitrophytic species) and water flows
833 (duration of wetness, nutrient supply; see Favero-Longo et al. 2023). As additional factors, (iii) the
834 possible persistence of epilithic and/or endolithic viable remains, favoured by (iv) the absence of an
835 effective devitalization combined with the mechanical cleaning -as in the case of the brush
836 application of BiotinR, not repeated after the removal of lithobionts- further limited the cleaning
837 effectiveness and remarked the opportunity/necessity for restorers of *in situ*, ad-hoc assays to
838 calibrate devitalization treatments (Favero-Longo et al., 2017; Sanmartín et al., 2023). The
839 application of biocidal compounds as preservative treatment after cleaning turned to balance this
840 procedural defect, likely finalizing the devitalization of viable lithobiontic residuals. In particular,
841 such positive effect was shared by the application of benzalkonium chloride and their natural
842 alternatives -plant essential oils and usnic acid-, which similarly delayed recolonization dynamics.
843 However, (v) their preservative action was already ceased before two years from the cleaning. With
844 this regard, conservation studies still need to fully characterize the stability and environmental fate
845 of traditional and innovative biocidal chemicals applied on stone substrates, and the factors
846 involved (Pinna, 2022), thus contributing an experimental validation of their single or periodic

applications to limit lithobiontic recolonization and/or addressing technical adjustments. A prolonged preservative effect, still maintaining the rock less darkened than the uncleaned surfaces after four years, was already shown by the photocatalytic nanocrystalline anatase and the polysiloxane-based water repellent. The positive effect of this latter, in particular, further remarked the opportunity to interfere with the microenvironmental conditions favourable to lithobionts to effectively limit the recolonization.

In general, our findings indicated that the reduction of stone bioreceptivity by direct intervention, e.g. with a permanent or semi-permanent integration of external substances, should be better considered an integrative strategy only, to be addressed and calibrated when indirect control approaches to reduce the recolonization risk, e.g. by limiting shading and water run-off of engraved surfaces, have been already explored.

6. Acknowledgements

This work was carried out in the framework of the project "Monitoring of, and Good Practices for, the protection of UNESCO site 94 Rock art in Valle Camonica", financed through law 77/2006 (financial year 2015) by the Italian Ministry of Cultural Heritage and Activities and Tourism. The cleaning of parcels was conducted thanks to the collaboration of the restorers Alessandro Danesi, Mari Mapelli, Antonella Sechi and Alessandro Segimiro. The authors are grateful to Emanuela Daffra (Director of Direzione regionale Musei Lombardia) and all the personnel of the Rock Engravings National Park of Naquane for logistic assistance during the field work and to Chiara Tonon and Chiara Michelis (University of Torino) for participation to some field activities.

7. References

Apprill, A., McNally, S., Parsons, R., Weber, L., 2015. Minor revision to V4 region SSU rRNA 806R gene primer greatly increases detection of SAR11 bacterioplankton. Aquat. Microb. Ecol. 75, 129-137. https://doi.org/10.3354/ame01753

Bartolini, M., Pietrini, A.M., Ricci, S., 2007. Valutazione dell'efficacia di alcuni nuovi biocidi per il trattamento di microflora fotosintetica e di briofite su materiali lapidei. Bollettino ICR (nuova serie) 14, 101-111.

Baruffo, L., Tretiach, M., 2007. Seasonal variations of F_0, F_m, and F_v/F_m in an epiphytic population of the lichen *Punctelia subrudecta* (Nyl.) Krog. Lichenologist 39, 555-565. https://doi.org/10.1017/S0024282907006846

Batarda Fernandes, A., Marshall, M., Domingo, I., 2022. Global Perspectives for the Conservation and Management of Open-Air Rock Art Sites. Routledge, London. https://doi.org/10.4324/9780429355349

Begora, M, Fahselt, D. 2001. Photolability of secondary compounds in some lichen species. Symbiosis 31, 3-22. http://hdl.handle.net/10222/77782

Bjelland, T., Kjeldsen, G., 2020. Status quo, ongoing challenges, and future perspectives-after more than 20 years of practice in rock art documentation, conservation, and management in southwestern Norway. Adoranten 2020, 1-12. https://hdl.handle.net/11250/3040348

Bjelland, T., Helberg, B.H., 2006. Rock Art. A guide to the documentation, management, presentation and monitoring of Norwegian Rock Art. The Directorate for Cultural Heritage, Oslo. http://hdl.handle.net/11250/226512

Bolyen, E., Rideout, J.R., Dillon, M.R. et al., 2019. Reproducible, interactive, scalable and extensible microbiome data science using QIIME 2. Nat Biotechnol 37, 852–857. https://doi.org/10.1038/s41587-019-0209-9

Borderie, F., Tête, N., Cailhol, D., Alaoui-Sehmer, L., Bousta, F., Rieffel, D., Aleya, L., Alaoui-Sossé, B., 2014. Factors driving epilithic algal colonization in show caves and new insights into combating biofilm development with UV-C treatments. Sci. Total Environ. 484, 43-52. https://doi.org/10.1016/j.scitotenv.2014.03.043

Bowker, M.A., Reed, S. C., Belnap, J., Phillips, S.L., 2002. Temporal variation in community composition, pigmentation, and F_v/F_m of desert cyanobacterial soil crusts. Microb. Ecol. 43, 13-25. https://doi.org/10.1007/s00248-001-1013-9

Brack, P., Dal Piaz, G.V., Baroni, C., Carton, A., Nardin, M., Pellegrini, G.B., Pennacchioni, G., 2008. Note illustrative della Carta Geologica d'Italia alla scala 1: 50.000. Foglio 058, Monte Adamello. Carta Geologica d'Italia alla scala 1: 50.000. ISPRA, Roma.

Callahan, B.J., McMurdie, P. J., Rosen, M. J., Han, A. W., Johnson, A.J.A., Holmes, S.P., 2016. DADA2: High-resolution sample inference from Illumina amplicon data. Nat. Methods 13, 581-583. https://doi.org/10.1038/nmeth.3869

Caneva, G., Nugari, M.P., Salvadori, O., 2008. Plant biology for cultural heritage: biodeterioration and conservation. Getty Publications, Los Angeles.

Caneva, G., Bartoli, F., Ceschin, S., Salvadori, O., Futagami, Y., Salvati, L., 2015. Exploring ecological relationships in the biodeterioration patterns of Angkor temples (Cambodia) along a forest canopy gradient. J. Cult. Herit. 16, 728-735. https://doi.org/10.1016/j.culher.2015.01.001

Cappitelli, F., Villa, F., 2021. Novel antibiofilm non-biocidal strategies, in: Joseph, E. (Ed.), Microorganisms in the deterioration and preservation of Cultural Heritage. Springer Nature, Cham, pp. 117-136. e, https://doi.org/10.1007/978-3-030-69411-1_5

915 Cappitelli, F., Cattò, C., Villa, F., 2020. The control of cultural heritage microbial deterioration.
916 Microorganisms 8, 1542. https://doi.org/10.3390/microorganisms8101542

917 Delgado Rodrigues, J., Anjos, M.V., Charola, A.E., 2011. Recolonization of marble sculptures in a
918 garden environment, in: Charola, A.E., McNamara, C., Koestler, R. (Eds.), Biocolonization of
919 stone: Control and preventive methods. Smithsonian contributions to museum conservation, 2.
920 Smithsonian Institution Scholarly Press, Washington, pp. 71-85.

921 de los Ríos, A., Pérez-Ortega, S., Wierzchos, J., & Ascaso, C., 2012. Differential effects of biocide
922 treatments on saxicolous communities: Case study of the Segovia cathedral cloister (Spain). Int.
923 Biodeter. Biodegr. 67, 64-72. doi.org/10.1016/j.ibiod.2011.10.010

924 Devreux, G., Santamaria, U., Morresi, F., Rodolfo, A., Barbabietola, N., Fratini, F., Reale, R., 2015.
925 Fitoconservazione, trattamenti alternativi sulle opere in materiale lapideo nei Giardini Vaticani.
926 In: Lo Stato dell'Arte XIII, Atti del XIII Congresso IGIIC, Torino, 24-26 ottobre 2015. Nardini
927 Editore, Firenze, pp. 199-206.

928 Favero-Longo, S.E., Viles, H.A., 2020. A review of the nature, role and control of lithobionts on
929 stone cultural heritage: Weighing-up and managing biodeterioration and bioprotection. World J.
930 Microbiol. Biotech. 36, 1-18. https://doi.org/10.1007/s11274-020-02878-3

931 Favero-Longo, S.E., Vannini, A., Benesperi, R., Bianchi, E., Fačkovcová, Z., Giordani, P.,
932 Malaspina, P., Martire, L., Matteucci, E., Paoli, L., Roccardi, A., Tonon, C., Loppi, S., 2020. The
933 application protocol impacts the effectiveness of biocides against lichens. Int. Biodeter. Biodegr.
934 155, 105105. doi.org/10.1016/j.ibiod.2020.105105

935 Favero-Longo, S.E., Benesperi, R., Bertuzzi, S., Bianchi, E., Buffa, G., Giordani, P., Loppi, S.,
936 Malaspina, P., Matteucci, E., Paoli, L., Ravera, S., Roccardi, A., Segimiro, A., Vannini, A., 2017.
937 Species-and site-specific efficacy of commercial biocides and application solvents against lichens.
938 Int. Biodeter. Biodegr. 123, 127-137. doi.org/10.1016/j.ibiod.2017.06.009

939 Favero-Longo, S.E., Matteucci, E., Pinna, D., Ruggiero, M.G., Riminesi, C., 2021. Efficacy of the
940 environmentally sustainable microwave heating compared to biocide applications in the
941 devitalization of phototrophic communities colonizing rock engravings of Valle Camonica,
942 UNESCO world heritage site, Italy. Int. Biodeter. Biodegr. 165, 105327.
943 https://doi.org/10.1016/j.ibiod.2021.105327

944 Favero-Longo, S.E., Matteucci, E., Castelli, D., Iacomussi, P., Martire, L., Ruggiero, M.G.,
945 Segimiro, A., 2023. An ecological investigation on lichens and other lithobionts colonizing rock
946 art in Valle Camonica (UNESCO WHS n. 94) addresses preventive conservation strategies.
947 Lichenologist, in press.

948 Favero-Longo, S.E., Castelli, D., Salvadori, O., Belluso, E., Piervittori, R., 2005. Pedogenetic
949 action of the lichens *Lecidea atrobrunnea*, *Rhizocarpon geographicum* gr. and *Sporastatia*
950 *testudinea* on serpentinized ultramafic rocks in an alpine environment. Int. Biodeter. Biodegr. 56,
951 17-27. doi.org/10.1016/j.ibiod.2004.11.006

952 Fidanza, M.R., Caneva, G., 2019. Natural biocides for the conservation of stone cultural heritage: A
953 review. J. Cult. Herit. 38, 271-286. doi.org/10.1016/j.culher.2019.01.005

954 Fonseca, A. J., Pina, F., Macedo, M. F., Leal, N., Romanowska-Deskins, A., Laiz, L., Gómez-
955 Bolea, A., Saiz-Jimenez, C., 2010. Anatase as an alternative application for preventing
956 biodeterioration of mortars: Evaluation and comparison with other biocides. Int. Biodeter.
957 Biodegr. 64, 388-396. https://doi.org/10.1016/j.ibiod.2010.04.006

958 Gabriele, F., Ranaldi, R., Bruno, L., Casieri, C., Rugnini, L., & Spreti, N., 2023. Biodeterioration of
959 stone monuments: Studies on the influence of bioreceptivity on cyanobacterial biofilm growth and
960 on the biocidal efficacy of essential oils in natural hydrogel. Sci. Total Environ. 870, 161901.
961 https://doi.org/10.1016/j.scitotenv.2023.161901

962 Gallo, C., Rizzo, P., Guerra, G., 2020. Antimicrobial release from cleaning poultices for the
963 conservation and disinfection of stone surfaces. Appl. Clay Sci. 193, 105667.
964 https://doi.org/10.1016/j.clay.2020.105667

965 Gazzano, C., Favero-Longo, S.E., Matteucci, E., Piervittori, R., 2009. Image analysis for measuring
966 lichen colonization on and within stonework. Lichenologist 41, 299-313.
967 https://doi.org/10.1017/S0024282909008366

968 Gazzano, C., Favero-Longo, S. E., Iacomussi, P., Piervittori, R., 2013. Biocidal effect of lichen
969 secondary metabolites against rock-dwelling microcolonial fungi, cyanobacteria and green algae.
970 Int. Biodeter. Biodegr. 84, 300-306. https://doi.org/10.1016/j.ibiod.2012.05.033

971 Goffredo, G. B., Accoroni, S., Totti, C., Romagnoli, T., Valentini, L., Munafò, P., 2017. Titanium
972 dioxide based nanotreatments to inhibit microalgal fouling on building stone surfaces. Build.
973 Environ. 112, 209-222. https://doi.org/10.1016/j.buildenv.2016.11.034

974 Gromaire, M. C., Van de Voorde, A., Lorgeoux, C., Chebbo, G., 2015. Benzalkonium runoff from
975 roofs treated with biocide products–In situ pilot-scale study. Water Res. 81, 279-287.
976 https://doi.org/10.1016/j.watres.2015.05.060

977 Guillitte, O.,1995. Bioreceptivity: a new concept for building ecology studies. Sci. Total Environ.
978 167, 215-220. https://doi.org/10.1016/0048-9697(95)04582-L

979 Hueck, H.J., 1965. The biodeterioration of materials as part of hylobiology. Mater. Organismen 1,
980 5-34.

981 ISO/CIE 11664-4, 2019. Colorimetry — Part 4: CIE 1976 L*a*b* colour space.

982 Jurado, V., Miller, A. Z., Cuezva, S., Fernandez-Cortes, A., Benavente, D., Rogerio-Candelera, M.
983 A., Reyes, J., Cañaveras, J.C., Sanchez-Moral, S., Saiz-Jimenez, C., 2014. Recolonization of
984 mortars by endolithic organisms on the walls of San Roque church in Campeche (Mexico): A case

985 of tertiary bioreceptivity. Constr. Build. Mater., 53, 348-359.
986 https://doi.org/10.1016/j.conbuildmat.2013.11.114

987 Konsta, A., Della Torre, S., 2021. Risk management and built heritage: Towards a systematic
988 approach, in: Roca, P., Pelà, L., Molins, C. (Eds.), SAHC 2021 - 12th International conference on
989 structural analysis of historical constructions. International Centre for Numerical Methods in
990 Engineering (CIMNE), Barcelona, pp. 3498-3509.

991 Li, T., Hu, Y., Zhang, B., 2020. Evaluation of efficiency of six biocides against microorganisms
992 commonly found on Feilaifeng Limestone, China. J. Cult. Herit. 43, 45-50.
993 https://doi.org/10.1016/j.culher.2019.11.006

994 Marques, J., Hespanhol, H., Paz-Bermúdez, G., Almeida, R., 2014. Choosing between sides in the
995 battle for pioneer colonization of schist in the Côa Valley Archaeological Park: a community
996 ecology perspective. J. Archaeol. Sci. 45, 206-216. https://doi.org/10.1016/j.jas.2014.02.021

997 Marques, J., Gonçalves, J., Oliveira, C., Favero-Longo, S.E., Paz-Bermúdez, G., Almeida, R.,
998 Prieto, B., 2016. On the dual nature of lichen-induced rock surface weathering in contrasting
999 micro-environments. Ecology 97, 2844-2857. https://doi.org/10.1002/ecy.1525

1000 McDonald, D., Price, M.N., Goodrich, J., Nawrocki, E.P., DeSantis, T.Z., Probst, A., et al. 2012.
1001 An improved Greengenes taxonomy with explicit ranks for ecological and evolutionary analyses
1002 of bacteria and archaea. ISME J. 6, 610–618. https://doi.org/10.1038/ismej.2011.139

1003 Morando, M., Matteucci, E., Nascimbene, J., Borghi, A., Piervittori, R., Favero-Longo, S.E., 2019.
1004 Effectiveness of aerobiological dispersal and microenvironmental requirements together influence
1005 spatial colonization patterns of lichen species on the stone cultural heritage. Sci. Total Environ.
1006 685, 1066-1074. doi.org/10.1016/j.scitotenv.2019.06.238

1007 Nascimbene, J., Salvadori, O., Nimis, P.L., 2009. Monitoring lichen recolonization on a restored
1008 calcareous statue. Sci. Total Environ. 407, 2420-2426.
1009 https://doi.org/10.1016/j.scitotenv.2008.12.037

1010 Nimis, P.L., Martellos, S., 2020. Towards a digital key to the lichens of Italy. Symbiosis 82, 149-
1011 155. https://doi.org/10.1007/s13199-020-00714-8

1012 Nimis, P.L., 2023. ITALIC - The Information System on Italian Lichens. Version 7.0. University of
1013 Trieste, Dept. of Biology. https://dryades.units.it/italic (accessed 16 April 2023)

1014 Parada, A.E., Needham, D.M., Fuhrman, J.A., 2015. Every base matters: Assessing small subunit
1015 rRNA primers for marine microbiomes with mock communities, time series and global field
1016 samples. Environ. Microbiol. 18, 1403–1414. https://doi.org/10.1111/1462-2920.13023

1017 Paz-Bermúdez, G., Prieto, B., Pozo-Antonio, J.S., 2023. Laser cleaning vs. chemical cleaning for
1018 Removal of lichen from schist surfaces in the Coa Valley (Portugal) and Siega Verde (Spain)
1019 archaeological sites, in: Batarda-Fernandes, A., Marshall, M., Domingo, I. (Eds.), Global
1020 perspectives for the conservation and management of open-air rock art sites. Routledge, London,
1021 pp. 177-193. https://doi.org/10.4324/9780429355349

1022 Pinna, D., 2017. Coping with biological growth on stone heritage objects: methods, products,
1023 applications, and perspectives. CRC Press, Boca Raton.

1024 Pinna, D., 2021. Microbial growth and its effects on inorganic heritage materials. In: Joseph, E.
1025 (Ed.) Microorganisms in the Deterioration and Preservation of Cultural Heritage. Springer Nature,
1026 Cham, pp. 3-35.

1027 Pinna, D., 2022. Can we do without biocides to cope with biofilms and lichens on stone heritage?.
1028 Int. Biodeter. Biodegr. 172, 105437. https://doi.org/10.1016/j.ibiod.2022.105437

1029 Pinna, D., Galeotti, M., Perito, B., Daly, G., Salvadori, B., 2018. In situ long-term monitoring of
1030 recolonization by fungi and lichens after innovative and traditional conservative treatments of

archaeological stones in Fiesole (Italy). Int. Biodeter. Biodegr. 132, 49-58. https://doi.org/10.1016/j.ibiod.2018.05.003

Pozo-Antonio, J.S., Barreiro, P., Paz-Bermúdez, G., González, P., Fernandes, A.B, 2021. Effectiveness and durability of chemical-and laser-based cleanings of lichen mosaics on schists at archaeological sites. Int. Biodeter. Biodegr. 163, 105276. https://doi.org/10.1016/j.ibiod.2021.105276

Rishbeth, J., 1948. The flora of Cambridge walls. J. Ecol. 36, 136-148. https://doi.org/10.2307/2256651

Ruggiero, L., Bartoli, F., Fidanza, M. R., Zurlo, F., Marconi, E., Gasperi, T., Tuti, S., Crociani, L., Di Bartolomeo, E., Caneva, G., Ricci, M.A., Sodo, A., 2020. Encapsulation of environmentally-friendly biocides in silica nanosystems for multifunctional coatings. Appl. Surf. Sci. 514, 145908. https://doi.org/10.1016/j.apsusc.2020.145908

Ruggiero, M.G., Basile, W., Favero-Longo, S.E., Matteucci, E., Quirino, T., Talarico, F., Torre, M., 2021. Il secondo progetto di monitoraggio dell'arte rupestre della Valle Camonica: Nuovi dati sulla distribuzione territoriale e sugli aspetti conservativi. BCSP 45: Proceedings of XXVII Valcamonica Symposium, pp. 145-155.

Salvadori, O., Charola, A.E., 2011. Methods to prevent biocolonization and recolonization: an overview of current research for architectural and archaeological heritage, in: Charola, A.E., McNamara, C., Koestler, R. (Eds.), Biocolonization of stone: Control and preventive methods. Smithsonian contributions to museum conservation, 2. Smithsonian Institution Scholarly Press, Washington, pp. 71-85.

Sanmartín, P., Fuentes, E., Montojo, C., Barreiro, P., Paz-Bermúdez, G., Prieto, B., 2019. Tertiary bioreceptivity of schists from prehistoric rock art sites in the Côa Valley (Portugal) and Siega Verde (Spain) archaeological parks: Effects of cleaning treatments. International Biodeterioration & Biodegradation 142, 151-159. doi.org/10.1016/j.ibiod.2019.05.011

1056 Sanmartín, P., Rodríguez, A., Aguiar, U., 2020. Medium-term field evaluation of several widely
1057 used cleaning-restoration techniques applied to algal biofilm formed on a granite-built historical
1058 monument. Int. Biodeter. Biodegr. 147, 104870. https://doi.org/10.1016/j.ibiod.2019.104870

1059 Sanmartín, P., Carballeira, R., 2021. Changes in heterotrophic microbial communities induced by
1060 biocidal treatments in the Monastery of San Martiño Pinario (Santiago de Compostela, NW
1061 Spain). Int. Biodeter. Biodegr. 156, 105130. https://doi.org/10.1016/j.ibiod.2020.105130

1062 Sanmartín, P., Miller, A. Z., Prieto, B., Viles, H.A., 2021a. Revisiting and reanalysing the concept
1063 of bioreceptivity 25 years on. Sci. Total Environ. 770, 145314.
1064 https://doi.org/10.1016/j.scitotenv.2021.145314

1065 Sanmartín, P., Noya-Pintos, D., Fuentes, E., Pozo-Antonio, J.S., 2021b. Cracks in consolidants
1066 containing TiO_2 as a habitat for biological colonization: A case of quaternary bioreceptivity.
1067 Mater. Sci. Eng. C 124, 112058. https://doi.org/10.1016/j.msec.2021.112058

1068 Sanmartín, P., Bosch-Roig, P., Pangallo, D., Kraková, L., Serrano, M., 2023. Unraveling disparate
1069 roles of organisms, from plants to bacteria, and viruses on built cultural heritage. Appli.
1070 Microbiol. Biotech. 107, 2027-2037. https://doi.org/10.1007/s00253-023-12423-5

1071 Scheerer, S., Ortega- Morales, O., Gaylarde, C., 2009. Microbial deterioration of stone
1072 monuments—an updated overview. Adv. Appl. Microbiol. 66, 97-139.
1073 https://doi.org/10.1016/S0065-2164(08)00805-8

1074 Scheidegger, C., Werth, S., 2009. Conservation strategies for lichens: insights from population
1075 biology. Fungal Biol. Rev. 23, 55-66. https://doi.org/10.1016/j.fbr.2009.10.003

1076 Spada, M., Cuzman, O. A., Tosini, I., Galeotti, M., Sorella, F., 2021. Essential oils mixtures as an
1077 eco-friendly biocidal solution for a marble statue restoration. Int. Biodet. Biodegr. 163, 105280.
1078 doi.org/10.1016/j.ibiod.2021.105280

Stirbet, A., Lazár, D., Papageorgiou, G.C., 2019. Chlorophyll a fluorescence in cyanobacteria: relation to photosynthesis, in: Mishra, A.K., Tiwari, D.N., Rai, A.N. (Eds.), Cyanobacteria. Academic Press, Cambridge (MA), pp. 79-130. https://doi.org/10.1016/B978-0-12-814667-5.00005-2

Tratebas, A.M., 2004. Biodeterioration of Prehistoric rock art and issues in site preservation. In: Seaward, M.R.D., St. Clair, L.L. (Eds.), Biodeterioration of stone surfaces. Springer, Dordrecht, pp. 195-228. https://doi.org/10.1007/978-1-4020-2845-8_12

Trojer, M. A., Nordstierna, L., Bergek, J., Blanck, H., Holmberg, K., Nydén, M., 2015. Use of microcapsules as controlled release devices for coatings. Adv. Colloid Interfac. 222, 18-43. https://doi.org/10.1016/j.cis.2014.06.003

Voyron, S., Tonon, C., Guglielmone, L., Celi, L., Comina, C., Ikeda, H., Matsumoto,., Petrella, D., Ryan, J., Sato, K., Seike, A., Varriale, I., Yamashita, J., Favero-Longo, S.E., Bonifacio, E., 2022. Diversity and structure of soil fungal communities unveil the building history of a burial mound of ancient Japan (Tobiotsuka Kofun, Okayama Prefecture). J. Archaeol. Sci. 146, 105656. https://doi.org/10.1016/j.jas.2022.105656

Young, G.S., Wainwright, I.N., 1995. The control of algal biodeterioration of a marble petroglyph site. Stud. Conserv. 40, 82-92. https://doi.org/10.1179/sic.1995.40.2.82

Zerboni, A., Villa, F., Wu, Y. L., Solomon, T., Trentini, A., Rizzi, A., Cappitelli, F., Gallinaro, M., 2022. The sustainability of rock art: preservation and Research. Sustainability 14, 6305. https://doi.org/10.3390/su14106305

Table captions

Table 1. Summary of the generalized linear model examining the effect of predictors (cleaning treatment, zone, year of monitoring, season of monitoring) on the fluorimetric parameters F_v/F_m and F_0.

Table 2. Monitoring of basal fluorescence (F0) in relationships with cleaning treatments. (A) Values quantified, at the different monitoring time points, for the cleaned parcels, separately considered for each treatment (codes are detailed in the main text and in Fig. 2), and the untreated surfaces between them (N-CON). Per each treatment, data are reported as av. values ± SE calculated for the three zones considered altogether (TOTAL) and separately (z3, z2, z1). Per each monitoring time point, values not sharing capital letters are significantly different (ANOVA with post-hoc Tukey's test; $P<0.05$), values significantly lower than control (N-CON) are underlined, and the lowest value(s) are marked in bold. (B) Percentage of measuring points displaying zeroed F_0 values. Values higher than 50% are underlined; per each monitoring time point, the highest value is marked in bold. n.d., not determined because of Covid-19 pandemic.

Table 3. Lichen recolonization detailed per each parcel in terms of (A) general occurrence after 37 (#) and 54 (##) months [*, colonization detected after 37 months, but disappeared after 54] and (B) specific occurrence with respect to T_0 after 54 months (-, absence of species detected at T_0; =, regrowth of species detected at T_0; +, appearance of a species not observed at T_0; reports of species observed after 37 months and disappeared after 54 are in brackets). Data are also summarized in terms of (C) total specific occurrence of each species throughout the parcels, after 54 months, and (D) per zone, after 54 and 37 months, and in terms of (E) variation of total specific occurrence after 54 months with respect to T0 (Δ sp. occ %), further detailed as regrowth in the same parcel (Recol. %) and new appearance (New occ. %). Codes of treatments are described in Material and Methods; nitrophytic species usually found as epiphytic are marked (§).

Figure captions

Fig. 1. Study site and monitored rock-art surfaces. (A) Localization of the Rock Engravings National Park of Naquane (red dot) in Capo di Ponte (Valle Camonica, Italy). (B-C) Rock 30 before (B) and immediately after (C) the cleaning of 27 parcels, oriented from north (z3, in the foreground) to south (z1, in the background). (D) Lithobiontic community on the rock surface (representative image from a parcel before its cleaning), including a cyanobacteria-dominated biofilm (cb; microscopic image in E, scale bar: 100 μm), foliose (fo.l) and crustose (cr.l) lichens, and mosses (m).

Fig. 2. Schematic experimental design: (A) zones z3-z1, primarily differing in shading levels, distributed from the northern to the southern side of Rock 30, each including a series of nine parcels; (B) conservative treatments assayed in the nine parcels of each zone [BAC, benzalkonium chloride; USN, usnic acid; SIL, polysiloxane-based water repellent; EST, water repellent and consolidant based on silicic acid ethyl esters and oligomeric polysiloxanes; EOL, essential oils; NTI, nanocrystalline anatase; uncleaned areas between the parcels of each zone, indicated as black bands in the scheme, were considered as negative controls, N-CON]; (C) monitoring time points and analyses performed through the 54 months monitoring program (*, fluorimetric measurements randomly performed through the parcels, before the adoption of the systematic sampling using the plastic mask).

Fig. 3. Recolonization patterns monitored by visual observations and image analysis. (A-C) Parcels of zones z3 (A), z2 (B), and z1 (C) on October 2020, 29 months after the cleaning intervention: the parcel boundaries were still recognizable in z3 and z2 (parcel codes detailed in main text), while the cyanobacterial and moss recolonization already made the parcels scarcely recognizable in z1. (D) Moss cover (%) quantified by image analysis for the three zones (z1-z3; av. ±SE values of the nine parcels of each zone). Per each monitoring time point, columns which do not share at least one lowercase letter are statistically different (superscripts $^{i\text{-}vi}$ mark letters related to the different time

points; ANOVA with Turkey's test. P<0.05); with reference to z1, columns which do not share at least one capital letter –below the x-axis- are significantly different; with reference to z2, only the cover calculated before the cleaning intervention is significantly different from the others (ANOVA with post-hoc Tukey's test, P<0.05). (E-H) Parcel considered before the cleaning (April 2018; E), immediately after (May 2018; F), after 25 (June 2020; G) and 54 months (November 2022; H), showing recolonization by lichens growing from the external border of the parcel (#) and in its central part (*, crustose thalli; §, sparse foliose lobes of *Xanthoparmelia*; magnified images in Fig. S4).

Fig. 4. Maximum quantum efficiency of Photosystem II (F_v/F_m; A-B) and basal fluorescence (F_0; C-D) quantified, at each monitoring time point, in (B-D) and between (controls; A-C) the cleaned parcels of the different zones (z1/z3). In B and D, boxes dealing with cleaned parcels at the summer time points (wide trellis pattern) significantly different from control areas (A-C) are marked with an asterisk (ANOVA with t-test; P <0.05). Per each Summer time point, box-plots related to the different zones which do not share at least one letter are statistically different (superscripts $^{i\text{-}iii}$ mark letters related to the different time points; ANOVA with Tukey's test, P<0.05).

Fig. 5. Lightness (L*) values of the parcels of z3 (white boxes) and z2 (grey boxes) after 37 (June 2021, A) and 49 (June 2022, B) months from the cleaning intervention, quantified in areas free of mosses (and debris) and expressed as difference from L* values of related uncleaned and unprotected areas. JUC, freshly cleaned parcels; other treatment codes are detailed in the main text. For each zone, box plots not sharing at least one letter are statistically different (z3, capital letters; z2, lowercase letters; ANOVA with post-hoc Tukey's test; P<0.05).

Tables

Table 1. Summary of the generalized linear model examining the effect of predictors (cleaning treatment, zone, year of monitoring, season of monitoring) on the fluorimetric parameters F_v/F_m and F_0.

Parameter	Source	Sum of squares	df	Mean-Square	F-Ratio	P
F_v/F_m	Treatment	1844398.252	9	204933.139	117.375	0.000
	Zone	24691.966	2	12345.983	7.071	0.001
	Year	2958431.825	3	986143.942	564.813	0.000
	Season	2573835.167	2	1286917.584	737.081	0.000
	Error	1.41214×10^7	8088	1745.965		
F_0	Treatment	44.825	9	4.981	92.987	0.000
	Zone	5.864	2	2.932	54.212	0.000
	Year	110.878	3	36.959	683.343	0.000
	Season	182.918	2	91.459	1690.991	0.000
	Error	437.339	8086	0.054		

Table 2. Monitoring of basal fluorescence (F_0) in relationships with cleaning treatments. (A) Values quantified, at the different monitoring time points, for the cleaned parcels, separately considered for each treatment (codes are detailed in the main text and in Fig. 2), and the untreated surfaces between them (N-CON). Per each treatment, data are reported as av. values ± SE calculated for the three zones considered altogether (TOTAL) and separately (z3, z2, z1). Per each monitoring time point, values not sharing capital letters are significantly different (ANOVA with post-hoc Tukey's test; $P<0.05$), values significantly lower than control (N-CON) are underlined, and the lowest value(s) are marked in bold. (B) Percentage of measuring points displaying zeroed F_0 values. Values higher than 50% are underlined; per each monitoring time point, the highest value is marked in bold. n.d., not determined because of Covid-19 pandemic.

	A	Jul-18	Oct-18	Mar-19	Jun-19	Oct-19	Mar-20	Jun-20	Oct-20	Mar-21	Jun-21	Oct-21
TOTAL	N-CON	49.2±4.1 A	57.9±5.0 A	37.1±3.2 A	52.3±4.4 A	52.8±3.7 A	n.d.	59.8±4.6 A	58.1±4.0 A	50.7±4.9 A	63.6±5.5 A	76.6±5.4 AB
	A-BAC	11.1±1.5 BC	13.8±1.7 BC	12.2±1.6 BCD	20.0±2.2 BCD	23.9±3.0 BCD	n.d.	35.0±3.4 BCD	38.4±2.4 B	38.1±2.4 AB	56.6±7.9 AB	64.1±3.1 ABC
	B-USN	7.7±1.2 BC	10.8±1.7 BC	8.0±1.1 CD	14.9±1.7 CD	17.9±1.6 CD	n.d.	39.2±2.7 BCD	38.2±1.9 B	40.1±2.6 AB	49.6±3.0 AB	65.0±2.8 ABC
	B-BAC	12.2±1.9 BC	12.9±1.5 BC	8.8±0.9 CD	15.9±1.5 CD	22.0±1.8 BCD	n.d.	36.1±2.8 BCD	38.3±2.6 B	**35.7±1.9** B	50.9±3.6 AB	65.9±3.9 ABC
	B-SIL	19.1±1.8 B	24.4±2.5 B	22.1±1.7 B	29.9±1.7 B	34.1±2.0 B	n.d.	44.7±1.5 BC	45.6±2.6 AB	37.6±2.4 AB	**43.7±2.5** B	57.8±3.6 BC
	B-EST	12.4±1.4 BC	15.3±1.5 BC	15.9±1.3 BC	22.0±1.6 BC	29.4±1.9 BC	n.d.	42.6±1.6 BCD	44.8±2.5 B	40.2±1.9 AB	51.8±2.3 AB	79.9±5.1 A
	B-EOL	**1.7±0.4** C	**5.1±3.0** C	**4.9±0.9** D	**7.4±0.6** D	**15.6±1.4** D	n.d.	28.1±1 D	44.8±2.2 B	38.5±2.1 AB	53.2±3.8 AB	**54.1±3.1** C
	B-NTI	19.7±1.8 B	24.6±2.4 B	15.2±1.3 BC	19.6±1.7 BCD	24.9±2.5 BCD	n.d.	29.1±1.9 CD	34.2±3.6 B	**34.9±3.5** B	46.7±4.6 AB	**53.4±4.7** C
	B-CON	15.3±1.7 B	25.7±2.9 B	16.5±1.9 BC	20.7±2.1 BC	26.9±2.3 BCD	n.d.	34.0±2.8 BCD	35.9±3.0 B	37.3±3.0 AB	51.1±4.5 AB	57.4±4.1 BC
	A-CON	11.1±1.1 BC	16.1±1.7 BC	13.1±1.3 BCD	20.2±1.9 BCD	31.3±3.6 B	n.d.	47.7±4.8 AB	39.6±4.2 B	41.6±4.1 AB	45.4±4.9 AB	59.4±6.8 ABC
z3	N-CON	55.5±10.3 A	55.13±9.2 A	34.1±5.1 A	62±11.7 A	47.9±7.5 A	n.d.	64.1±10.2 A	71.4±9.5 A	83.7±13.0 A	88.5±13.4 A	105.6±12.7 A
	A-BAC	5.3±1.5 B	10.2±3 B	9.3±3.4 B	14.3±2.9 B	13.6±1.9 B	n.d.	35.1±4.4 BC	42.1±3.8 B	46.8±3.9 B	88.1±22.4 AB	69.8±6.4 ABC
	B-USN	8.5±2.8 B	9.9±3.6 B	5.6±1.7 B	9.1±2.3 B	10.2±2-0 B	n.d.	31.1±3.9 BC	35.8±2.8 B	41.5±3.0 B	54.7±5.5 ABC	60.3±2.9 BC
	B-BAC	4.3±1.5 B	6.0±1.9 B	2.6±0.5 B	6.2±1.2 B	6.1±1.2 B	n.d.	17.4±2.7 BC	21.2±2.3 B	23.7±1.8 B	43.9±8.1 BC	**50.1±6.2** C
	B-SIL	12.6±1.9 B	11.2±2.1 B	14.7±2.1 B	16.9±2.3 B	16.7±2.0 B	n.d.	41.4±2.1 AB	45.7±2.7 B	44.5±2.8 B	51.0±2.1 ABC	59.1±3.7 BC
	B-EST	4.3±0.9 B	5.9±1.2 B	10.3±1.9 B	8.1±1.0 B	11.3±1.4 B	n.d.	36.0±3.0 BC	44.4±2.6 B	44.5±2.5 B	61.2±2.2 ABC	94.7±7.5 AB
	B-EOL	3.3±1.1 B	11.9±8.7 B	2.1±0.3 B	6.6±0.7 B	8.7±0.7 B	n.d.	24.7±1.5 BC	44.9±1.9 B	44.9±2.4 B	56.6±1.5 ABC	72.0±2.7 BC
	B-NTI	10.8±2 B	12.7±2.9 B	9.0±2.1 B	9.4±1.7 B	8.6±1.7 B	n.d.	16.2±1.3 BC	22.2±2.6 B	27.7±3.0 B	**28.1±2.4** C	**44.2±3.1** C
	B-CON	4.7±1.4 B	5.9±1.9 B	1.2±0.3 B	3.7±0.7 B	8.0±1.6 B	n.d.	**13.7±2.8** C	20.6±2.1 B	28.2±3.1 B	**32.1±2.5** C	**52.6±2.9** C
	A-CON	6.7±1.1 B	10.3±2.5 B	8.6±2.4 B	9.3±1.4 B	12.9±1.9 B	n.d.	22.8±3.5 BC	35.3±5.5 B	36.2±4.1 B	54.2±5.5 ABC	74.9±5.6 ABC
z2	N-CON	54.4±5.1 A	73.5±9.8 A	51.4±6.8 A	59.5±4.4 A	59.6±6.5 A	n.d.	60.6±6.8 A	56.9±5.3 AB	40.1±2.3 BC	63.5±6.8 AB	75.5±6.7 ABC
	A-BAC	5.5±1.0 BCD	6.2±1.7 C	3.7±0.9 BC	9.2±2.5 D	15.6±3.5 DE	n.d.	**20.7±2.4** E	36.5±4.7 BCD	30.9±3.1 CDE	36.6±2.8 C	68.2±5.1 ABCD
	B-USN	5.2±0.8 CD	9.1±1.5 C	8.8±1.5 BC	16.9±2.9 D	19.9±2.8 CDE	n.d.	51.1±5.4 ABCD	44.7±3.1 ABCD	45.9±2.2 AB	64.9±3.9 AB	86.2±3.4 AB
	B-BAC	9.5±1.8 BCD	12±1.9 C	10.4±1.3 BC	15.7±1.7 D	26.1±2.4 BCDE	n.d.	55.6±4.3 AB	60.7±3.3 A	52.3±1.6 A	74.6±2.7 A	99.7±2.9 A
	B-SIL	15.8±2.1 BCD	21.5±3.9 BC	18.2±1.9 BC	37.9±2.5 B	38.8±1.6 BC	n.d.	53.5±1.9 ABC	51.1±1.5 ABC	35.8±1.4 BCD	40.0±1.6 C	58.5±3.9 BCD
	B-EST	22.4±2.7 B	22.4±2.4 BC	22.5±2.2 B	35.3±2.7 B	41.0±2.5 B	n.d.	52.7±2.5 ABC	46.4±1.1 ABCD	36.5±1.2 BCD	46.1±1.5 BC	54.2±2.2 CD
	B-EOL	**1.0±0.2** D	1.2±0.2 C	**2.6±1.4** C	4.5±0.7 D	**8.3±1.2** E	n.d.	29.3±1.9 DE	39.0±2.2 CD	28.6±1.8 DE	32.9±1.7 C	52.4±2.1 CD
	B-NTI	16.5±3.1 BCD	21.6±5.0 BC	13.7±2.4 BC	16.4±2.6 D	16.7±2.7 DE	n.d.	31.4±3.6 CDE	**26.6±2.7** D	**23.7±2.1** E	35.1±1.9 C	**37.7±3.5** D
	B-CON	20.9±3.2 BC	39.1±5.4 B	23.2±3.2 B	33.1±4.3 BC	34.7±3.0 BCD	n.d.	43.3±3.0 ABCDE	36.5±2.5 CD	37.3±2.5 BCD	45.0±2.7 BC	**48.3±2.5** D
	A-CON	9.2±1.7 BCD	11.1±2.5 C	9.7±1.8 BC	19.2±2.7 CD	24±2.9 BCDE	n.d.	36.8±2.9 BCDE	47.0±8.2 ABCD	29.9±3.3 DE	36.4±2.1 C	65.6±15.2 BCD
z1	N-CON	36.5±4.5 A	42.3±5.5 A	23.3±2.8 BCD	33.7±4.8 AB	49.9±5.1 AB	n.d.	54.4±6.7 B	45.7±4.6 A	28.7±4.6 B	37.8±5.9 BC	47.3±5.2 BC
	A-BAC	20.1±2.7 BC	22.5±2.7 CDEF	20.8±1.9 BCDE	32.7±3.5 AB	38.6±5.9 ABCD	n.d.	45.4±7.1 BC	36.6±3.9 A	36.3±4.3 AB	45.5±5.0 ABC	56.3±4.2 ABC
	B-USN	9.6±2.2 CD	13.5±3.3 EF	**9.6±2.4** E	18.8±3.5 BC	**23.8±3.0** D	n.d.	34.6±3.5 BC	33.5±3.6 A	32.4±6.8 AB	27.8±2.7 C	47.0±4.6 BC
	B-BAC	24.0±4.9 ABC	21.6±2.9 CDEF	14±1.9 CDE	27.1±3.3 AB	35.2±2.4 BCD	n.d.	35.3±4.1 BC	32.2±3.2 A	30.3±3.4 AB	32.3±2.5 BC	45.7±4.8 BC
	B-SIL	29.5±4.1 AB	41.5±4.1 AB	33.9±3.4 A	34.7±1.8 A	47.1±3.1 ABC	n.d.	38.7±2.9 BC	39.5±7.5 A	32.3±6.5 AB	40.2±7.2 ABC	55.9±9.8 BC
	B-EST	11.4±1.9 CD	18.3±2.6 DEF	15.3±2.1 BCDE	23.6±1.2 ABC	36.9±2.1 ABCD	n.d.	39.7±1.9 BC	43.6±6.7 A	39.2±4.7 AB	47.6±5.7 ABC	88.7±11.5 A
	B-EOL	**0.9±0.2** D	**2±0.5** F	**10±2** E	**10.9±1.2** C	29.6±1.9 CD	n.d.	**30.2±1.4** C	50.1±5.8 A	41.6±5.0 AB	69.3±9.8 AB	37.6±7.4 C
	B-NTI	30.6±2.6 AB	38.4±3.0 ABC	22.3±1.6 BC	31.9±2.4 AB	47.1±3.5 ABC	n.d.	38.9±3.0 BC	51.7±8.6 A	51.1±8.3 AB	73.8±10.6 A	75.1±11.4 AB
	B-CON	21.0±3.1 BC	34.1±4.6 ABCD	26.2±3.0 AB	27.0±2.5 AB	39.0±3.8 ABCD	n.d.	46.5±5.0 BC	50.6±7.1 A	46.3±7.3 AB	75.2±11.0 A	70.1±10.7 ABC
	A-CON	17.4±2.1 BC	26.9±2.8 BCDE	21±1.9 BCDE	31.7±3.4 AB	56.8±8.1 A	n.d.	83.5±10.6 A	35.7±7.5 A	59.5±10.6 A	46.9±14.1 ABC	37.9±10.1 BC

	B	J-18	O-18	M-19	J-19	O-19	M-20	J-20	O-20	M-21	J-21	O-21
	N-CON	15.1	1.5	21.6	10.8	9.4	n.d.	5.0	2.2	8.6	5.0	4.3
	A-BAC	59.3	49.2	50.8	39.0	33.9	n.d.	5.1	0.0	5.1	0.0	1.7
	B-USN	74.4	65.4	71.8	48.7	41.0	n.d.	2.6	3.8	3.8	3.8	3.8
	B-BAC	61.5	57.7	62.8	42.3	32.1	n.d.	12.8	2.6	5.1	1.3	2.6
	B-SIL	32.0	37.3	17.3	10.7	4.0	n.d.	1.3	0.0	5.3	0.0	1.3
	B-EST	53.2	41.8	39.2	25.3	17.7	n.d.	0.0	0.0	2.5	3.8	0.0
	B-EOL	**98.8**	**95.0**	**88.8**	**72.5**	**47.5**	n.d.	0.0	1.3	1.3	0.0	3.8
	B-NTI	36.8	34.2	40.8	32.9	34.7	n.d.	7.9	12.0	**16.0**	5.3	**9.3**
	B-CON	53.2	44.2	49.4	41.6	31.2	n.d.	**13.0**	5.2	9.1	3.9	5.2
	A-CON	52.9	44.3	44.3	30.0	22.9	n.d.	8.6	**11.4**	10.0	**10.1**	7.1
z3	N-CON	20.0	0.0	35.6	13.3	17.8	n.d.	2.2	0.0	0.0	0.0	0.0
	A-BAC	78.9	63.2	68.4	47.4	42.1	n.d.	0.0	0.0	0.0	0.0	0.0
	B-USN	80.8	76.9	88.5	69.2	65.4	n.d.	0.0	0.0	0.0	0.0	0.0
	B-BAC	85.2	85.2	96.3	81.5	**88.9**	n.d.	25.9	3.7	3.7	0.0	0.0
	B-SIL	44.0	72.0	36.0	32.0	12.0	n.d.	0.0	0.0	4.0	0.0	0.0
	B-EST	92.6	77.8	63.0	70.4	51.9	n.d.	0.0	0.0	0.0	0.0	0.0
	B-EOL	**96.3**	**88.9**	**100.0**	77.8	63.0	n.d.	0.0	0.0	0.0	0.0	0.0
	B-NTI	56.0	60.0	76.0	64.0	72.0	n.d.	12.0	**20.0**	**12.0**	**8.0**	0.0
	B-CON	88.9	85.2	**100.0**	**96.3**	77.8	n.d.	**37.0**	11.1	3.7	0.0	0.0
	A-CON	72.7	59.1	68.2	59.1	54.5	n.d.	18.2	0.0	0.0	0.0	0.0
z2	N-CON	7.8	2.0	9.8	3.9	2.0	n.d.	3.9	0.0	2.0	2.0	2.0
	A-BAC	88.2	82.4	88.2	76.5	52.9	n.d.	**11.8**	0.0	0.0	0.0	0.0
	B-USN	77.8	63.0	66.7	40.7	33.3	n.d.	0.0	0.0	0.0	0.0	0.0
	B-BAC	63.0	63.0	51.9	29.6	3.7	n.d.	0.0	0.0	0.0	0.0	0.0
	B-SIL	23.1	26.9	15.4	0.0	0.0	n.d.	0.0	0.0	0.0	0.0	0.0
	B-EST	12.0	16.0	8.0	4.0	0.0	n.d.	0.0	0.0	0.0	0.0	0.0
	B-EOL	**100.0**	**100.0**	**96.2**	**92.3**	**76.9**	n.d.	0.0	0.0	0.0	0.0	0.0
	B-NTI	50.0	41.7	45.8	37.5	34.8	n.d.	8.3	**4.3**	**17.4**	0.0	0.0
	B-CON	34.8	21.7	26.1	17.4	8.7	n.d.	0.0	0.0	4.3	0.0	0.0
	A-CON	60.0	60.0	60.0	24.0	12.0	n.d.	4.0	4.0	4.0	**4.0**	**4.0**
z1	N-CON	18.6	2.3	20.9	16.3	9.3	n.d.	9.3	7.0	25.6	14.0	11.6
	A-BAC	21.7	13.0	8.7	4.3	13.0	n.d.	4.3	0.0	13.0	0.0	4.3
	B-USN	64.0	56.0	60.0	36.0	**24.0**	n.d.	8.0	12.0	12.0	12.0	12.0
	B-BAC	33.3	20.8	37.5	12.5	0.0	n.d.	**12.5**	4.2	12.5	4.2	8.3
	B-SIL	29.2	12.5	0.0	0.0	0.0	n.d.	4.2	0.0	12.5	0.0	4.2
	B-EST	51.9	29.6	44.4	0.0	0.0	n.d.	0.0	0.0	7.4	11.1	0.0
	B-EOL	**100.0**	**96.3**	**70.4**	**48.1**	3.7	n.d.	0.0	3.7	3.7	0.0	11.1
	B-NTI	7.4	3.7	3.7	0.0	0.0	n.d.	3.7	11.1	18.5	7.4	25.9
	B-CON	33.3	22.2	18.5	7.4	3.7	n.d.	0.0	3.7	18.5	11.1	14.8
	A-CON	26.1	13.0	4.3	8.7	4.3	n.d.	4.3	**30.4**	**26.1**	**27.3**	**17.4**

Table 3. Lichen recolonization detailed per each parcel in terms of (A) general occurrence after 37 (#) and 54 (##) months [*, colonization detected after 37 months, but disappeared after 54] and (B) specific occurrence with respect to T_0 after 54 months (-, absence of species detected at T_0; =, regrowth of species detected at T_0; +, appearance of a species not observed at T_0; reports of species observed after 37 months and disappeared after 54 are in brackets). Data are also summarized in terms of (C) total specific occurrence of each species throughout the parcels, after 54 months, and (D) per zone, after 54 and 37 months, and in terms of (E) variation of total specific occurrence after 54 months with respect to T0 (Δ sp. occ %), further detailed as regrowth in the same parcel (Recol. %) and new appearance (New occ. %). Codes of treatments are described in Material and Methods; nitrophytic species usually found as epiphytic are marked (§).

Treatment	A-BAC	B-USN	B-BAC	B-SIL	B-EST	B-EOL	B-NTI	B-CON	A-CON	A-BAC	B-USN	B-BAC	B-SIL	B-EST	B-EOL	B-NTI	B-CON	A-CON	A-BAC	B-USN	B-BAC	B-SIL	B-EST	B-EOL	B-NTI	B-CON	A-CON			
Zone	3	3	3	3	3	3	3	3	3	2	2	2	2	2	2	2	2	2	1	1	1	1	1	1	1	1	1			
(a) Lichen recolonization	##	##	##	##	##	##	##	##	##	##	##	##	##	#	#	##	##	##	##	##	##	##	##	##	##	*	#			
(b) Specific recolonization																												**(c) Total specific occurrences**		
																												-	=	+
Candelaria concolor (Dicks.) Stein (§)	=	=	=	=	=					+		+											+	+	+			0	5	5
Candelariella vitellina (Hoffm.) Müll. Arg.							-		+	+	-			-	-		-											5	0	2
Cladonia sp.																							+					0	0	1
Circinaria caesiocinerea (Malbr.) A. Nordin, Savić & Tibell and/or *Fuscidea lygaea* (W. Mann) V. Wirth & Vězda)	=	=	-	=		=	=	=	=	=	+	=	=	=	=	+	=	+	=	+								1	14	4
Pertusaria flavicans Lamy			-	-	-					-								-		=	=		=	=	=	(=)		5	5	0
Phaeophyscia orbicularis (Neck.) Moberg (§)	+	=	=		=																				+		+	0	3	3
Physcia adscendens H. Olivier (§)	+	+	+		+	(+)	(+)		-								-					+						2	0	5
Rufoplaca gr. *arenaria* (Pers.) Arup, Søchting & Frödén	+		-	-	-	=	=	+	=	+	+	=	=	=	+	+	=	+	+		+	=		-			-	5	8	9
Greenish *Xanthoparmelia*	=	=	-	-	-	-		+	=	=	=	=	-	-	-	-	-	=	=		-		-	-				12	8	1
Xanthoparmelia glabrans (Nyl.) O. Blanco, A. Crespo, Elix, D. Hawksw. & Lumbsch	=	-							+		-	-	-		-	-	-	-			-							9	1	1
Total occurrences T_0	4	5	5	5	5	3	3	1	4	3	3	5	4	4	4	2	6	3	2	1	3	1	2	3	1	1	1			
Total occurrences $T4_{yrs}$	7	5	3	2	3	2	2	3	5	5	3	4	2	2	2	2	2	3	3	2	2	2	3	2	3	0	1			
Δ specific occurrences (T4yrs vs. T0; %)	75	0	-40	-60	-40	-33	-33	200	25	67	0	-20	-50	-50	-50	0	-67	0	50	100	-33	100	50	-33	200	-100	0			
Recolonizations (%)	57	80	33	100	67	100	100	33	60	40	33	75	100	100	50	0	100	33	67	50	50	50	33	50	33	-	0			
New occurrences (%)	43	20	67	0	33	0	0	67	40	60	67	25	0	0	50	100	0	67	33	50	50	50	67	50	67	-	100			

(d) Total specific occurrences per zone		-	=	+						-	=	+							-	=	+								
54 months	Z3	14	22	10						Z2	19	14	11						Z1	7	8	10								
[37 months	Z3	21	15	8						Z2	25	8	6						Z1	8	7	5]								

(e) Variation of specific occurrences per treatment		Δ sp. occ. (%)	Recol. (%)	New occ. (%)				Δ sp. occ. (%)	Recol. (%)	New occ. (%)			
54 months	A-CON	14	14	30	30	30	30	B-EOL	-39	10	67	29	33	29
	A-BAC	64	13	55	14	45	14	B-USN	33	58	54	24	46	24
	B-CON	11	164	67	47	33	47	B-SIL	-3	90	83	29	17	29
	B-BAC	-31	10	53	21	47	21	B-EST	-13	54	67	38	33	38
								B-NTI	56	126	44	51	56	51

Table 1. Summary of the generalized linear model examining the effect of predictors (cleaning treatment, zone, year of monitoring, season of monitoring) on the fluorimetric parameters F_v/F_m and F_0.

Parameter	Source	Sum of squares	df	Mean-Square	F-Ratio	P
F_v/F_m	Treatment	1844398.252	9	204933.139	117.375	0.000
	Zone	24691.966	2	12345.983	7.071	0.001
	Year	2958431.825	3	986143.942	564.813	0.000
	Season	2573835.167	2	1286917.584	737.081	0.000
	Error	1.41214×10^7	8088	1745.965		
F_0	Treatment	44.825	9	4.981	92.987	0.000
	Zone	5.864	2	2.932	54.212	0.000
	Year	110.878	3	36.959	683.343	0.000
	Season	182.918	2	91.459	1690.991	0.000
	Error	437.339	8086	0.054		

Table 2. Monitoring of basal fluorescence (F_0) in relationships with cleaning treatments. (A) Values quar surfaces between them (N-CON). Per each treatment, data are reported as av. values ± SE calculated fo hoc Tukey's test; $p<0.05$), values significantly lower than control (N-CON) are underlined, and the lowes marked in bold. n.d., not determined because of Covid-19 pandemic.

	A	Jul-18		Oct-18		Mar-19		Jun-19		Oct-19	
TOTAL	N-CON	49.2±4.1	A	57.9±5.0	A	37.1±3.2	A	52.3±4.4	A	52.8±3.7	A
	A-BAC	11.1±1.5	BC	13.8±1.7	BC	12.2±1.6	BCD	20.0±2.2	BCD	23.9±3.0	BCD
	B-USN	7.7±1.2	BC	10.8±1.7	BC	8.0±1.1	CD	14.9±1.7	CD	17.9±1.6	CD
	B-BAC	12.2±1.9	BC	12.9±1.5	BC	8.8±0.9	CD	15.9±1.5	CD	22.0±1.8	BCD
	B-SIL	19.1±1.8	B	24.4±2.5	B	22.1±1.7	B	29.9±1.7	B	34.1±2.0	B
	B-EST	12.4±1.4	BC	15.3±1.5	BC	15.9±1.3	BC	22.0±1.6	BC	29.4±1.9	BC
	B-EOL	**1.7±0.4**	C	**5.1±3.0**	C	**4.9±0.9**	D	**7.4±0.6**	D	**15.6±1.4**	D
	B-NTI	19.7±1.8	B	24.6±2.4	B	15.2±1.3	BC	19.6±1.7	BCD	24.9±2.5	BCD
	B-CON	15.3±1.7	B	25.7±2.9	B	16.5±1.9	BC	20.7±2.1	BC	26.9±2.3	BCD
	A-CON	11.1±1.1	BC	16.1±1.7	BC	13.1±1.3	BCD	20.2±1.9	BCD	31.3±3.6	B
z3	N-CON	55.5±10.3	A	55.13±9.2	A	34.1±5.1	A	62±11.7	A	47.9±7.5	A
	A-BAC	5.3±1.5	B	10.2±3	B	9.3±3.4	B	14.3±2.9	B	13.6±1.9	B
	B-USN	8.5±2.8	B	9.9±3.6	B	5.6±1.7	B	9.1±2.3	B	10.2±2-0	B
	B-BAC	4.3±1.5	B	6.0±1.9	B	2.6±0.5	B	6.2±1.2	B	6.1±1.2	B
	B-SIL	12.6±1.9	B	11.2±2.1	B	14.7±2.1	B	16.9±2.3	B	16.7±2.0	B
	B-EST	4.3±0.9	B	5.9±1.2	B	10.3±1.9	B	8.1±1.0	B	11.3±1.4	B
	B-EOL	3.3±1.1	B	11.9±8.7	B	2.1±0.3	B	6.6±0.7	B	8.7±0.7	B
	B-NTI	10.8±2	B	12.7±2.9	B	9.0±2.1	B	9.4±1.7	B	8.6±1.7	B
	B-CON	4.7±1.4	B	5.9±1.9	B	1.2±0.3	B	3.7±0.7	B	8.0±1.6	B
	A-CON	6.7±1.1	B	10.3±2.5	B	8.6±2.4	B	9.3±1.4	B	12.9±1.9	B
z2	N-CON	54.4±5.1	A	73.5±9.8	A	51.4±6.8	A	59.5±4.4	A	59.6±6.5	A
	A-BAC	5.5±1.0	BCD	6.2±1.7	C	3.7±0.9	BC	9.2±2.5	D	15.6±3.5	DE
	B-USN	5.2±0.8	CD	9.1±1.5	C	8.8±1.5	BC	16.9±2.9	D	19.9±2.8	CDE
	B-BAC	9.5±1.8	BCD	12±1.9	C	10.4±1.3	BC	15.7±1.7	D	26.1±2.4	BCDE
	B-SIL	15.8±2.1	BCD	21.5±3.9	BC	18.2±1.9	BC	37.9±2.5	B	38.8±1.6	BC
	B-EST	22.4±2.7	B	22.4±2.4	BC	22.5±2.2	B	35.3±2.7	B	41.0±2.5	B
	B-EOL	**1.0±0.2**	D	1.2±0.2	C	**2.6±1.4**	C	4.5±0.7	D	**8.3±1.2**	E
	B-NTI	16.5±3.1	BCD	21.6±5.0	BC	13.7±2.4	BC	16.4±2.6	D	16.7±2.7	DE
	B-CON	20.9±3.2	BC	39.1±5.4	B	23.2±3.2	B	33.1±4.3	BC	34.7±3.0	BCD
	A-CON	9.2±1.7	BCD	11.1±2.5	C	9.7±1.8	BC	19.2±2.7	CD	24±2.9	BCDE
z1	N-CON	36.5±4.5	A	42.3±5.5	A	23.3±2.8	BCD	33.7±4.8	AB	49.9±5.1	AB
	A-BAC	20.1±2.7	BC	22.5±2.7	CDEF	20.8±1.9	BCDE	32.7±3.5	AB	38.6±5.9	ABCD
	B-USN	9.6±2.2	CD	13.5±3.3	EF	**9.6±2.4**	E	18.8±3.5	BC	**23.8±3.0**	D
	B-BAC	24.0±4.9	ABC	21.6±2.9	CDEF	14±1.9	CDE	27.1±3.3	AB	35.2±2.4	BCD
	B-SIL	29.5±4.1	AB	41.5±4.1	AB	33.9±3.4	A	34.7±1.8	A	47.1±3.1	ABC
	B-EST	11.4±1.9	CD	18.3±2.6	DEF	15.3±2.1	BCDE	23.6±1.2	ABC	36.9±2.1	ABCD
	B-EOL	**0.9±0.2**	D	**2±0.5**	F	**10±2**	E	**10.9±1.2**	C	29.6±1.9	CD
	B-NTI	30.6±2.6	AB	38.4±3.0	ABC	22.3±1.6	BC	31.9±2.4	AB	47.1±3.5	ABC
	B-CON	21.0±3.1	BC	34.1±4.6	ABCD	26.2±3.0	AB	27.0±2.5	AB	39.0±3.8	ABCD
	A-CON	17.4±2.1	BC	26.9±2.8	BCDE	21±1.9	BCDE	31.7±3.4	AB	56.8±8.1	A

ıtified, at the different monitoring time points, for the cleaned parcels, separately considered for each treatme
r the three zones considered altogether (TOTAL) and separately (z3, z2, z1). Per each monitoring time point, va
ıt value(s) are marked in bold. (B) Percentage of measuring points displaying zeroed F_0 values. Values higher th

Mar-20	Jun-20	Oct-20	Mar-21	Jun-21	Oct-21	**B**
n.d.	59.8±4.6 A	58.1±4.0 A	50.7±4.9 A	63.6±5.5 A	76.6±5.4 AB	N-CON
n.d.	35.0±3.4 BCD	38.4±2.4 B	38.1±2.4 AB	56.6±7.9 AB	64.1±3.1 ABC	A-BAC
n.d.	39.2±2.7 BCD	38.2±1.9 B	40.1±2.6 AB	49.6±3.0 AB	65.0±2.8 ABC	B-USN
n.d.	36.1±2.8 BCD	38.3±2.6 B	**35.7±1.9** B	50.9±3.6 AB	65.9±3.9 ABC	B-BAC
n.d.	44.7±1.5 BC	45.6±2.6 AB	37.6±2.4 AB	**43.7±2.5** B	57.8±3.6 BC	B-SIL
n.d.	42.6±1.6 BCD	44.8±2.5 B	40.2±1.9 AB	51.8±2.3 AB	79.9±5.1 A	B-EST
n.d.	28.1±1 D	44.8±2.2 B	38.5±2.1 AB	53.2±3.8 AB	**54.1±3.1** C	B-EOL
n.d.	29.1±1.9 CD	34.2±3.6 B	**34.9±3.5** B	46.7±4.6 AB	**53.4±4.7** C	B-NTI
n.d.	34.0±2.8 BCD	35.9±3.0 B	37.3±3.0 AB	51.1±4.5 AB	57.4±4.1 BC	B-CON
n.d.	47.7±4.8 AB	39.6±4.2 B	41.6±4.1 AB	45.4±4.9 AB	59.4±6.8 ABC	A-CON
n.d.	64.1±10.2 A	71.4±9.5 A	83.7±13.0 A	88.5±13.4 A	105.6±12.7 A	N-CON
n.d.	35.1±4.4 BC	42.1±3.8 B	46.8±3.9 B	88.1±22.4 AB	69.8±6.4 ABC	A-BAC
n.d.	31.1±3.9 BC	35.8±2.8 B	41.5±3.0 B	54.7±5.5 ABC	60.3±2.9 BC	B-USN
n.d.	17.4±2.7 BC	21.2±2.3 B	23.7±1.8 B	43.9±8.1 BC	**50.1±6.2** C	B-BAC
n.d.	41.4±2.1 AB	45.7±2.7 B	44.5±2.8 B	51.0±2.1 ABC	59.1±3.7 BC	B-SIL
n.d.	36.0±3.0 BC	44.4±2.6 B	44.5±2.5 B	61.2±2.2 ABC	94.7±7.5 AB	B-EST
n.d.	24.7±1.5 BC	44.9±1.9 B	44.9±2.4 B	56.6±1.5 ABC	72.0±2.7 BC	B-EOL
n.d.	16.2±1.3 BC	22.2±2.6 B	27.7±3.0 B	**28.1±2.4** C	**44.2±3.1** C	B-NTI
n.d.	**13.7±2.8** C	20.6±2.1 B	28.2±3.1 B	**32.1±2.5** C	**52.6±2.9** C	B-CON
n.d.	22.8±3.5 BC	35.3±5.5 B	36.2±4.1 B	54.2±5.5 ABC	74.9±5.6 ABC	A-CON
n.d.	60.6±6.8 A	56.9±5.3 AB	40.1±2.3 BC	63.5±6.8 AB	75.5±6.7 ABC	N-CON
n.d.	**20.7±2.4** E	36.5±4.7 BCD	30.9±3.1 CDE	36.6±2.8 C	68.2±5.1 ABCD	A-BAC
n.d.	51.1±5.4 ABCD	44.7±3.1 ABCD	45.9±2.2 AB	64.9±3.9 AB	86.2±3.4 AB	B-USN
n.d.	55.6±4.3 AB	60.7±3.3 A	52.3±1.6 A	74.6±2.7 A	99.7±2.9 A	B-BAC
n.d.	53.5±1.9 ABC	51.1±1.5 ABC	35.8±1.4 BCD	40.0±1.6 C	58.5±3.9 BCD	B-SIL
n.d.	52.7±2.5 ABC	46.4±1.1 ABCD	36.5±1.2 BCD	46.1±1.5 BC	54.2±2.2 CD	B-EST
n.d.	29.3±1.9 DE	39.0±2.2 CD	28.6±1.8 DE	32.9±1.7 C	52.4±2.1 CD	B-EOL
n.d.	31.4±3.6 CDE	**26.6±2.7** D	**23.7±2.1** E	35.1±1.9 C	**37.7±3.5** D	B-NTI
n.d.	43.3±3.0 ABCDE	36.5±2.5 CD	37.3±2.5 BCD	45.0±2.7 BC	**48.3±2.5** D	B-CON
n.d.	36.8±2.9 BCDE	47.0±8.2 ABCD	29.9±3.3 DE	36.4±2.1 C	65.6±15.2 BCD	A-CON
n.d.	54.4±6.7 B	45.7±4.6 A	28.7±4.6 B	37.8±5.9 BC	47.3±5.2 BC	N-CON
n.d.	45.4±7.1 BC	36.6±3.9 A	36.3±4.3 AB	45.5±5.0 ABC	56.3±4.2 ABC	A-BAC
n.d.	34.6±3.5 BC	33.5±3.6 A	32.4±6.8 AB	27.8±2.7 C	47.0±4.6 BC	B-USN
n.d.	35.3±4.1 BC	32.2±3.2 A	30.3±3.4 AB	32.3±2.5 BC	45.7±4.8 BC	B-BAC
n.d.	38.7±2.9 BC	39.5±7.5 A	32.3±6.5 AB	40.2±7.2 ABC	55.9±9.8 BC	B-SIL
n.d.	39.7±1.9 BC	43.6±6.7 A	39.2±4.7 AB	47.6±5.7 ABC	88.7±11.5 A	B-EST
n.d.	**30.2±1.4** C	50.1±5.8 A	41.6±5.0 AB	69.3±9.8 AB	37.6±7.4 C	B-EOL
n.d.	38.9±3.0 BC	51.7±8.6 A	51.1±8.3 AB	73.8±10.6 A	75.1±11.4 AB	B-NTI
n.d.	46.5±5.0 BC	50.6±7.1 A	46.3±7.3 AB	75.2±11.0 A	70.1±10.7 ABC	B-CON
n.d.	83.5±10.6 A	35.7±7.5 A	59.5±10.6 A	46.9±14.1 ABC	37.9±10.1 BC	A-CON

ɛnt (codes are detailed in the main text and in Fig. 2), and the untreated
ılues not sharing capital letters are significantly different (ANOVA with post-
an 50% are underlined; per each monitoring time point, the highest value is

J-18	O-18	M-19	J-19	O-19	M-20	J-20	O-20	M-21	J-21	O-21
15.1	1.5	21.6	10.8	9.4	n.d.	5.0	2.2	8.6	5.0	4.3
59.3	49.2	50.8	39.0	33.9	n.d.	5.1	0.0	5.1	0.0	1.7
74.4	65.4	71.8	48.7	41.0	n.d.	2.6	3.8	3.8	3.8	3.8
61.5	57.7	62.8	42.3	32.1	n.d.	12.8	2.6	5.1	1.3	2.6
32.0	37.3	17.3	10.7	4.0	n.d.	1.3	0.0	5.3	0.0	1.3
53.2	41.8	39.2	25.3	17.7	n.d.	0.0	0.0	2.5	3.8	0.0
98.8	**95.0**	**88.8**	**72.5**	**47.5**	n.d.	0.0	1.3	1.3	0.0	3.8
36.8	34.2	40.8	32.9	34.7	n.d.	7.9	12.0	**16.0**	5.3	**9.3**
53.2	44.2	49.4	41.6	31.2	n.d.	**13.0**	5.2	9.1	3.9	5.2
52.9	44.3	44.3	30.0	22.9	n.d.	8.6	**11.4**	10.0	**10.1**	7.1
20.0	0.0	35.6	13.3	17.8	n.d.	2.2	0.0	0.0	0.0	0.0
78.9	63.2	68.4	47.4	42.1	n.d.	0.0	0.0	0.0	0.0	0.0
80.8	76.9	88.5	69.2	65.4	n.d.	0.0	0.0	0.0	0.0	0.0
85.2	85.2	96.3	81.5	**88.9**	n.d.	25.9	3.7	3.7	0.0	0.0
44.0	72.0	36.0	32.0	12.0	n.d.	0.0	0.0	4.0	0.0	0.0
92.6	77.8	63.0	70.4	51.9	n.d.	0.0	0.0	0.0	0.0	0.0
96.3	**88.9**	**100.0**	77.8	63.0	n.d.	0.0	0.0	0.0	0.0	0.0
56.0	60.0	76.0	64.0	72.0	n.d.	12.0	**20.0**	**12.0**	**8.0**	0.0
88.9	85.2	**100.0**	**96.3**	77.8	n.d.	**37.0**	11.1	3.7	0.0	0.0
72.7	59.1	68.2	59.1	54.5	n.d.	18.2	0.0	0.0	0.0	0.0
7.8	2.0	9.8	3.9	2.0	n.d.	3.9	0.0	2.0	2.0	2.0
88.2	82.4	88.2	76.5	52.9	n.d.	**11.8**	0.0	0.0	0.0	0.0
77.8	63.0	66.7	40.7	33.3	n.d.	0.0	0.0	0.0	0.0	0.0
63.0	63.0	51.9	29.6	3.7	n.d.	0.0	0.0	0.0	0.0	0.0
23.1	26.9	15.4	0.0	0.0	n.d.	0.0	0.0	0.0	0.0	0.0
12.0	16.0	8.0	4.0	0.0	n.d.	0.0	0.0	0.0	0.0	0.0
100.0	**100.0**	**96.2**	**92.3**	**76.9**	n.d.	0.0	0.0	0.0	0.0	0.0
50.0	41.7	45.8	37.5	34.8	n.d.	8.3	**4.3**	**17.4**	0.0	0.0
34.8	21.7	26.1	17.4	8.7	n.d.	0.0	0.0	4.3	0.0	0.0
60.0	60.0	60.0	24.0	12.0	n.d.	4.0	4.0	4.0	**4.0**	**4.0**
18.6	2.3	20.9	16.3	9.3	n.d.	9.3	7.0	25.6	14.0	11.6
21.7	13.0	8.7	4.3	13.0	n.d.	4.3	0.0	13.0	0.0	4.3
64.0	56.0	60.0	36.0	**24.0**	n.d.	8.0	12.0	12.0	12.0	12.0
33.3	20.8	37.5	12.5	0.0	n.d.	**12.5**	4.2	12.5	4.2	8.3
29.2	12.5	0.0	0.0	0.0	n.d.	4.2	0.0	12.5	0.0	4.2
51.9	29.6	44.4	0.0	0.0	n.d.	0.0	0.0	7.4	11.1	0.0
100.0	**96.3**	**70.4**	**48.1**	3.7	n.d.	0.0	3.7	3.7	0.0	11.1
7.4	3.7	3.7	0.0	0.0	n.d.	3.7	11.1	18.5	7.4	25.9
33.3	22.2	18.5	7.4	3.7	n.d.	0.0	3.7	18.5	11.1	14.8
26.1	13.0	4.3	8.7	4.3	n.d.	4.3	**30.4**	**26.1**	**27.3**	**17.4**

Table 3. Lichen recolonization detailed per each parcel in terms of (A) general occurrence after 37 (#) and 54 (##) month T0 after 54 months (-, absence of species detected at T0; =, regrowth of species detected at T0; +, appearance of a speci are also summarized in terms of (C) total specific occurrence of each species throughout the parcels, after 54 months, a with respect to T0 (Δ sp. occ %), further detailed as regrowth in the same parcel (Recol. %) and new appearance (New o are marked (§).

Treatment	A-BAC	B-USN	B-BAC	B-SIL	B-EST	B-EOL	B-NTI	B-CON	A-CON
Zone	3	3	3	3	3	3	3	3	3
(A) Lichen recolonization	##	##	##	##	##	##	##	##	##
(B) Specific recolonization									
Candelaria concolor (Dicks.) Stein (§)	=	=	=	=	=				
Candelariella vitellina (Hoffm.) Müll. Arg.							-		+
Cladonia sp.									
Circinaria caesiocinerea (Malbr.) A. Nordin, Savić & Tibell and/or *Fuscidea lygaea* (W. Mann) V. Wirth & Vězda)	=	=	-	=		=	=	=	=
Pertusaria flavicans Lamy			-	-	-				
Phaeophyscia orbicularis (Neck.) Moberg (§)	+	=	=		=				
Physcia adscendens H. Olivier (§)	+	+	+		+	(+)	(+)		-
Rufoplaca gr. *arenaria* (Pers.) Arup, Søchting & Frödén	+		-	-	-	=	=	+	=
Greenish *Xanthoparmelia*	=	=	-	-	-	-		+	=
Xanthoparmelia glabrans (Nyl.) O. Blanco, A. Crespo, Elix, D. Hawksw. & Lumbsch	=	-							+
Total occurrences T_0	4	5	5	5	5	3	3	1	4
Total occurrences $T4_{yrs}$	7	5	3	2	3	2	2	3	5
Δ specific occurrences (T4yrs vs. T0; %)	75	0	-40	-60	-40	-33	-33	200	25
Recolonizations (%)	57	80	33	100	67	100	100	33	60
New occurrences (%)	43	20	67	0	33	0	0	67	40

(D) Total specific occurrences per zone		-	=	+
54 months	z3	14	22	10
[37 months	z3	21	15	8

(E) Variation of specific occurrences per treatment		Δ sp. occ. (%)		Recol. (%)		New occ. (%)	
54 months	A-CON	14	14	30	30	30	30
	A-BAC	64	13	55	14	45	14
	B-CON	11	164	67	47	33	47
	B-BAC	-31	10	53	21	47	21

ıs [*, colonization detected after 37 months, but disappeared after 54] and (B) specific occurrence with respect to ies not observed at T0; reports of species observed after 37 months and disappeared after 54 are in brackets). Data nd (D) per zone, after 54 and 37 months, and in terms of (E) variation of total specific occurrence after 54 months cc. %). Codes of treatments are described in Material and Methods; nitrophytic species usually found as epiphytic

A-BAC	B-USN	B-BAC	B-SIL	B-EST	B-EOL	B-NTI	B-CON	A-CON	A-BAC	B-USN	B-BAC	B-SIL	B-EST	B-EOL	B-NTI	B-CON	A-CON			
2	2	2	2	2	2	2	2	2	1	1	1	1	1	1	1	1	1			
##	##	##	##	#	#	##	##	##	##	##	##	##	##	##	##	*	#			
																		(C) Total specific occurrences		
																		-	=	+
+		+											+	+	+			0	5	5
+	-			-	-		-											5	0	2
													+					0	0	1
																		1	14	4
=	+	=	=	=	=	+	=	+	=	+										
-								-		=	=		=	=	=	(=)		5	5	0
															+		+	0	3	3
							-					+						2	0	5
+	+	=	=	=	+	+	=	+	+		+	=		-			-	5	8	9
=	=	=	-	-	-	-	-	=	=		-		-	-				12	8	1
	-	-	-		-	-	-	-			-							9	1	1
3	3	5	4	4	4	2	6	3	2	1	3	1	2	3	1	1	1			
5	3	4	2	2	2	2	2	3	3	2	2	2	3	2	3	0	1			
67	0	-20	-50	-50	-50	0	-67	0	50	100	-33	100	50	-33	200	-100	0			
40	33	75	100	100	50	0	100	33	67	50	50	50	33	50	33	-	0			
60	67	25	0	0	50	100	0	67	33	50	50	50	67	50	67	-	100			
	-	=	+							-	=	+								
z2	19	14	11						z1	7	8	10								
z2	25	8	6						z1	8	7	5]								

	Δ sp. occ. (%)		Recol. (%)		New occ. (%)	
B-EOL	-39	10	67	29	33	29
B-USN	33	58	54	24	46	24
B-SIL	-3.3	90	83	29	17	29
B-EST	-13	54	67	38	33	38
B-NTI	56	126	44	51	56	51

Figure 1

Click here to access/download;Figure;Figura 1rev_b.tif

Figure 2

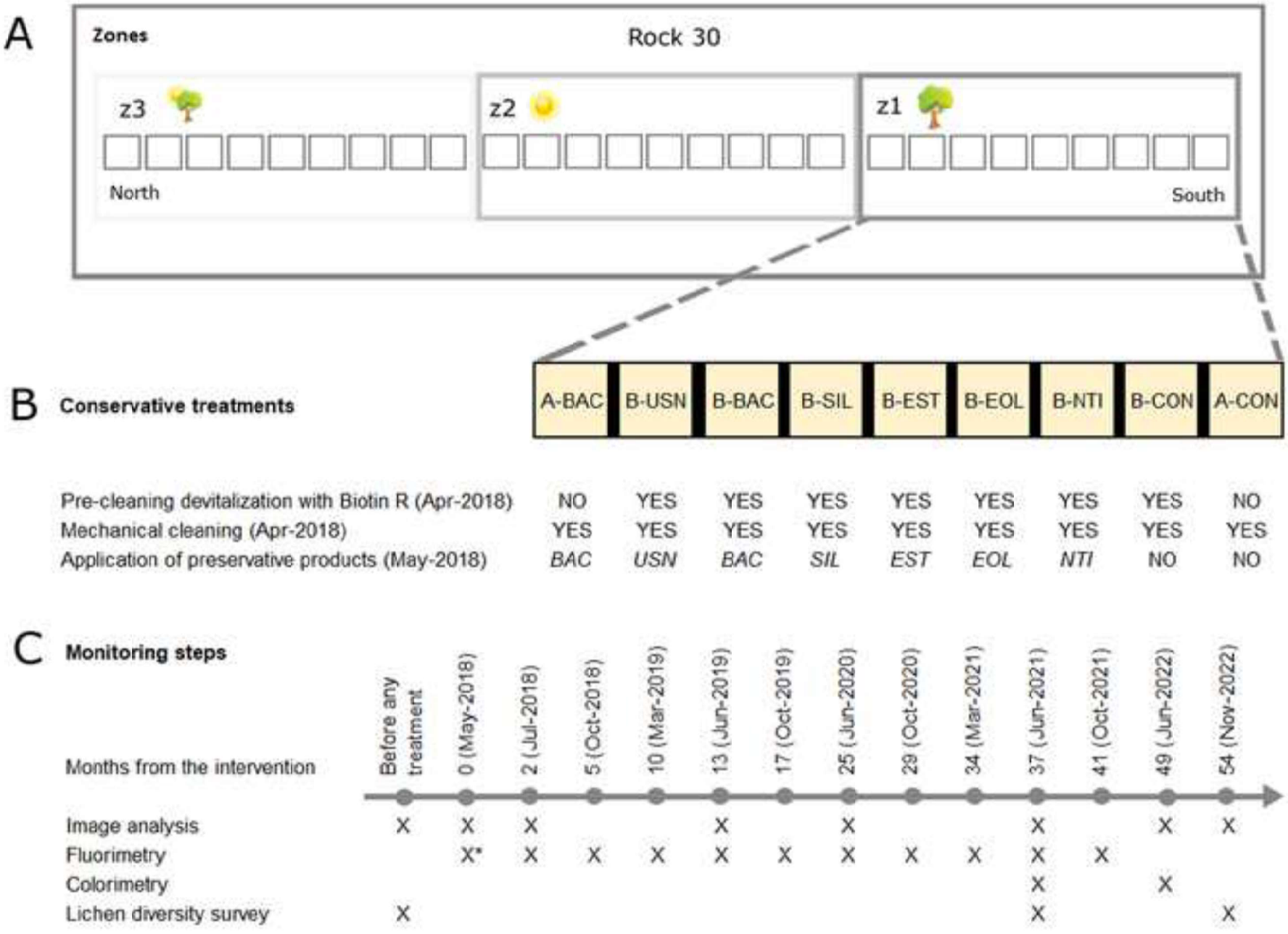

Figure 3

Click here to access/download;Figure;Favero-Longo et al. - Fig.3.tif

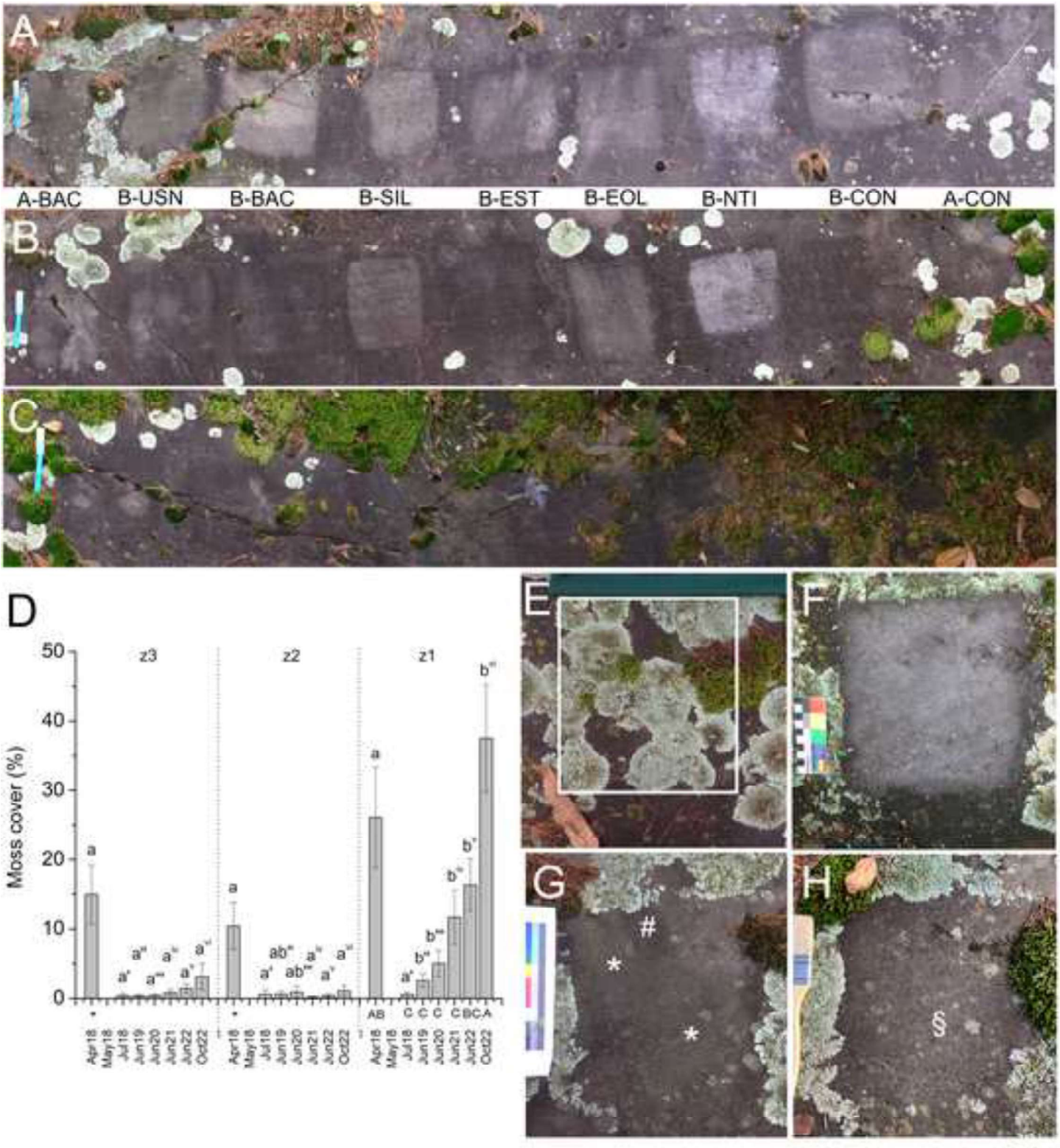

Figure 4

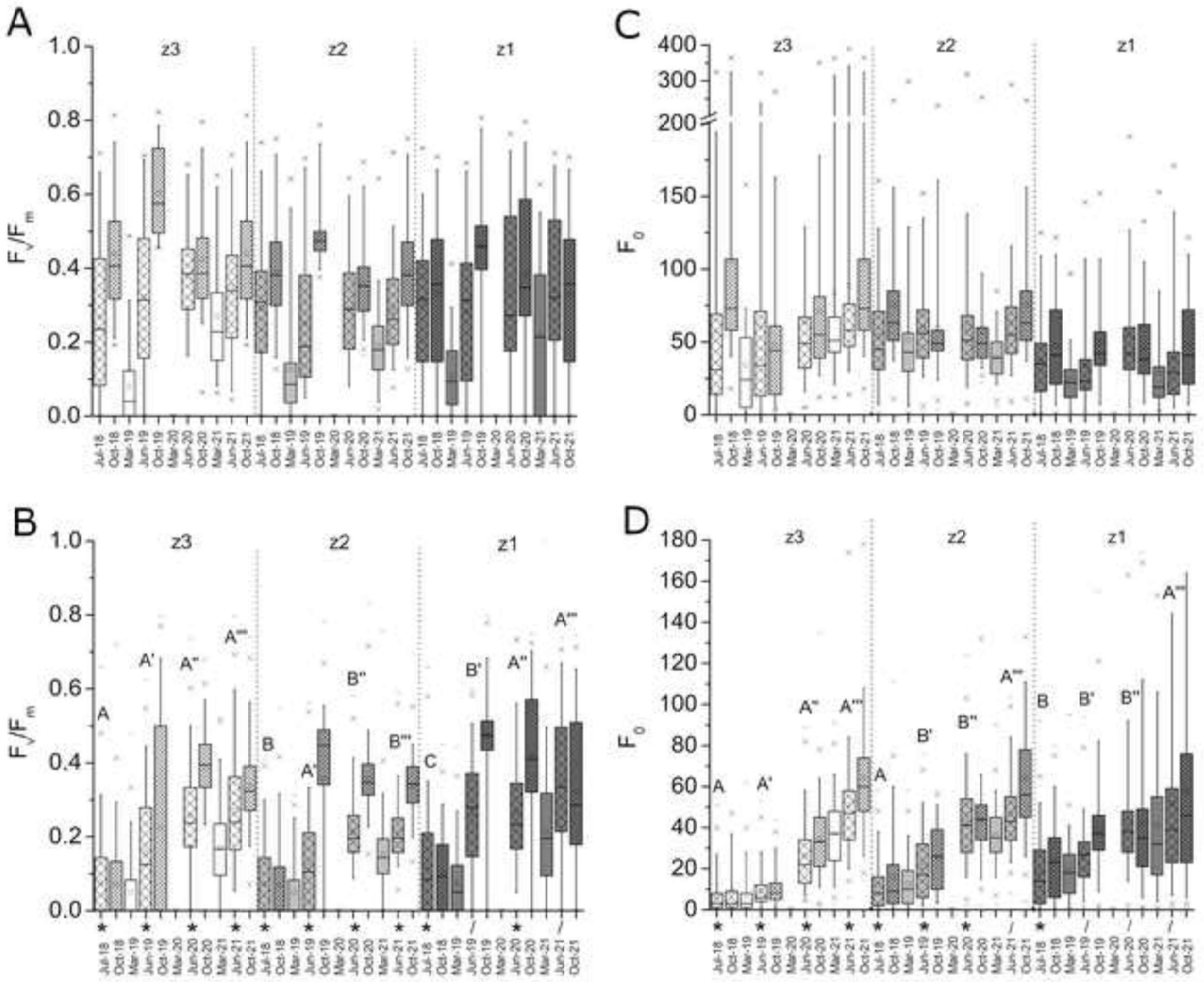

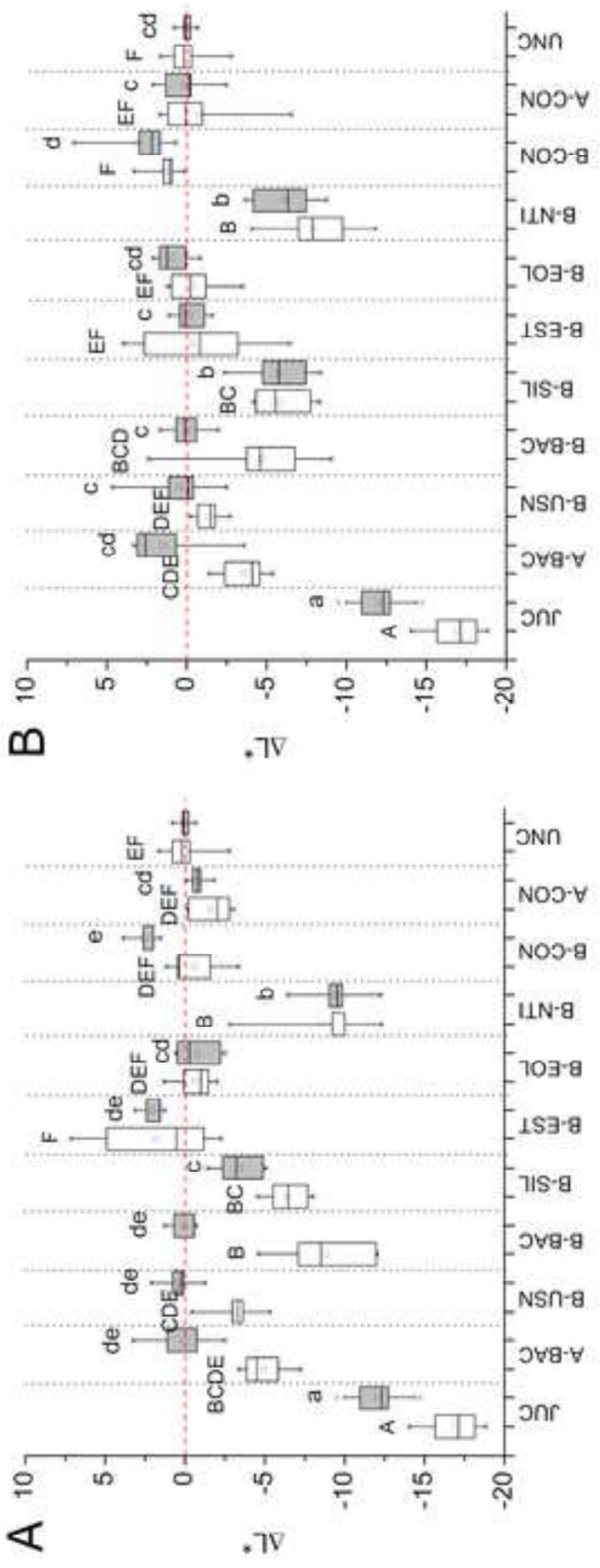

Figure 5

Supplementary Material (Tables S1-S2; Figs. S1, S3-S6)

Fig. S2

Declaration of interests

☒The authors declare that they have no known competing financial interests or personal relationships that could have appeared to influence the work reported in this paper.

☐The authors declare the following financial interests/personal relationships which may be considered as potential competing interests:

Author Contributions Statement

S.E. F-L., E. M. and M.G. R. conceived the project; M.G. R. provided research funds; S.E F-L. and E. M. carried out field activities and analyzed images and fluorimetric data; S. V. carried out molecular analyses; P. I. analyzed colorimetric data; S.E. F-L. wrote the manuscript with support from all the co-authors; S.E. and M.G. R. supervised the project